

<http://researchcommons.waikato.ac.nz/>

## **Research Commons at the University of Waikato**

### **Copyright Statement:**

The digital copy of this thesis is protected by the Copyright Act 1994 (New Zealand).

The thesis may be consulted by you, provided you comply with the provisions of the Act and the following conditions of use:

- Any use you make of these documents or images must be for research or private study purposes only, and you may not make them available to any other person.
- Authors control the copyright of their thesis. You will recognise the author's right to be identified as the author of the thesis, and due acknowledgement will be made to the author where appropriate.
- You will obtain the author's permission before publishing any material from the thesis.

**Do benthic macrofauna functional groups or their key  
constituent species better predict variation in ecosystem  
functioning?**

A thesis

submitted in partial fulfilment

of the requirements for the degree of

**Master of Science (Research) in Biological Sciences**

at

**The University of Waikato**

by

**Grady Petersen**



THE UNIVERSITY OF  
**WAIKATO**  
*Te Whare Wānanga o Waikato*

2018

# Abstract

---

Estuarine ecosystems are important zones for primary productivity and nutrient processing, have rich communities of plants and animals and support important fisheries and are fundamental to food webs. Intertidal habitats in estuaries are highly dynamic environments, subject to tidal variation and often have strong environmental gradients of salinity, turbidity and bed sediment grain size. These environmental factors contribute to the diversity of macrofaunal assemblages which vary over a range of spatial and temporal scales. This study was based in the Manukau Harbour, New Zealand, and aimed to investigate the spatial variation of nutrient processing within the harbour, and whether this variation is best explained by biotic or abiotic variables. Additionally, DistLM models were employed to find if either macrofauna functional groups or key species in these groups serve as better predictors of ecosystem function.

To provide empirical information to a project designing a whole-estuary nutrient mixing model, a team of ecologists deployed benthic incubation chambers (0.25 m<sup>2</sup>) to measure solute fluxes, and assessed the macrofauna community and sediment characteristics at 6 intertidal sandflat sites in the Manukau Harbour over a 4 day period in December 2016. Denitrification rates were measured at 2 sites to provide information on nitrogen removal from the harbour. This thesis deals specifically with how the macrofaunal communities and how they relate to and influence nutrient fluxes.

Macrofauna collected from the Manukau Harbour were assigned functional groups based on species specific traits. Multiple regression models were performed using functional groups and ecosystem variables as predictors, and

dark chamber fluxes of  $O_2$ ,  $NH_4^+$  and  $NO_x^-$  as response variables. Significantly correlated functional groups ( $p < 0.05$ ) were substituted for their constituent species to determine whether functional groups or individual species served as better predictors of ecosystem functioning.

The results indicated that while functional groups may provide redundancy in terms of multiple species carrying out similar functional roles, there are key species that dominate these roles. In addition to the macrofauna functional groups, several environmental variables (mud content, phaeophytin biomass and organic content) served as important predictors for changes in ecosystem functioning.

This suggests that macrofauna functional groups form complex relationships with environmental variables which influence ecosystem functioning through benthic metabolism and excretion and macrofaunally-mediated such as bioturbation and irrigation of sediments. These biological processes alter the oxic-anoxic boundaries and facilitate the breakdown and remineralisation of deposited organic matter, fuelling primary productivity and nitrogen cycling.

At two sites where denitrification was measured, the total amount of nitrogen leaving the water column was similar ( $242.3$  and  $234.8 \mu\text{mol N m}^{-2} \text{ h}^{-1}$ ), however the rates of denitrification of these sites was significantly ( $p = 0.0001$ ) different, suggesting that permanent removal of nitrogen varies spatially across the harbour, which can have important connotations for ecosystem management.

# Acknowledgements

---

I would like to thank all the people who have helped me throughout the process of my masters for their help, encouragement and support.

Firstly, I'd like to give a big thanks to my supervisors Conrad Pilditch (University of Waikato) and Drew Lohrer (NIWA) for their guidance, support and seemingly endless knowledge on all things marine ecology. Your time and effort has certainly kept the stress away and helped me create a piece of work am proud of.

Thank you to NIWA for providing me with this opportunity and inspiring me to pursue my interest in marine sciences. Thank you to the benthos team for all their help and the use of their lab, resources and knowledge. Water chemistry analysis and various field work costs were covered by a Watercare Services Ltd. contract to NIWA (project no. WSL16205; Manukau Harbour hydrodynamic and water quality models). Big thanks to Barry and Sarah for teaching me how to ID macrofauna, Lisa for helping me with chlorophyll samples, Kelly for helping me with grain size, and anyone who checked my sorting and data sheets. Thanks to Mike T, Drew, Lisa, Kelly, Sarah, Sam, Mike MY, Kit and Scotty for making the fieldwork easy, fun and memorable. Additional thanks to Barry for proofreading and giving feedback. Thank you to Rebecca for checking and helping me with IDs and for teaching me how to use Primer, and thanks again to Drew for teaching me how to use SAS.

I'd like to thank my mother for her endless love and support in everything I do, and my friends, family and lovely girlfriend for putting up with my ramblings about worms, nitrogen and mud. Thank you to everyone for showing interest (or at least

pretending, no matter how unconvincing) in my thesis and encouraging me throughout the whole process. Thank you to everyone at UNI and NIWA for morning coffees and chats, they're one of the most important parts of writing a thesis. And a huge thanks to everyone who shouted me a beer during my time as a student, you've been the biggest help.

In summary, thanks to all of those involved in giving me this this opportunity, funding elements of my thesis, and providing me with the tools, knowledge and skills needed to complete this undertaking.

Cheers team.

# Table of Contents

---

Abstract .....	i
Acknowledgements.....	iii
Table of Contents .....	v
Table of Figures .....	vii
Table of Tables .....	ix
1. Introduction .....	1
2. Methods.....	13
2.1 Study area.....	13
2.2 Study design .....	16
2.3 In situ chamber incubations .....	18
2.4 Sampling of environmental variables.....	21
2.5 Laboratory analyses.....	21
2.6 Functional groups .....	22
2.7 Flux calculations and data analysis.....	26
3. Results.....	30
3.1 Environmental variables and macrofauna .....	30
3.2 Nutrient fluxes.....	38
3.2.1 Benthic metabolism .....	38
3.2.2 Nutrient regeneration .....	41
3.3 Functional groups or species as predictors of ecosystem function .....	49
3.4 Denitrification.....	55
4. Discussion .....	57
4.1 Predictors of ecosystem function.....	57
4.2 Solute fluxes .....	63
4.3 Environmental controls of macrofauna .....	66

4.4	Denitrification.....	68
4.5	Modelling and extrapolation.....	71
4.6	Future work.....	72
5.	Conclusion.....	74
	References.....	76
	Appendices.....	89



# Table of Figures

Figure 1.1: A) Simplified diagram showing cycling of nitrogen and removal of nitrogen in benthic-pelagic coupling and B) Graphic representation of nitrogen cycling in the water column, oxic and anoxic sediments.....	6
Figure 2.1: Map of the Manukau Harbour showing the locations of study sites ( <i>CH</i> Cape Horn, <i>PI</i> Pahurehure Inlet, <i>AA</i> Auckland Airport, <i>KP</i> Karaka Point, <i>EB</i> Elliot's Beach, and <i>CB</i> Clarks Beach) and the catchment area of the harbour (all water within the dark orange highlighted area flows into the harbour). Source: <a href="http://www.watercare.co.nz">www.watercare.co.nz</a> . ....	14
Figure 2.2: A) Before and B) after the removal of oxidation settling ponds in the north-eastern area of the Manukau Harbour. Source: Iain Henderson, New Zealand Geographic. ....	15
Figure 2.3: A) The base of the flux chamber pressed into the sediment. 1) Water pump, 2) dissolved oxygen logger with HOBO data logger, 3) battery pack for water pump. B) Paired chambers with lids and shade cloth attached and sampling tubes connected after inundation. Note: DO and HOBO logger attached to the outside of the light chamber to measure the external water DO concentrations. Source: NIWA archives, 2016. ....	19
Figure 3.1: Non-metric Multi-dimensional scaling (nMDS) (Bray-Curtis resemblance) of benthic macrofauna community composition expressed as (A) raw species data and (B) functional group abundance at each site. Each of the points on this plot indicate a single sediment core sample, and the different colours denote the six different sites	35
Figure 3.2: Principle coordinate analysis (Bray-Curtis similarity) of macrofauna (Log(X+1) transformed) community expressed as (A) raw species data and (B) functional group data at each site with vector overlay of select environmental variables known to be important in structuring macrofaunal communities. ....	37
Figure 3.3: (A) Mean ( $\pm$ SE) dissolved O <sub>2</sub> flux at each site ( $\square$ = light chamber/NPP, $\blacksquare$ = dark chamber/SOC). (B) Mean gross primary productivity at each site, with a secondary axis of mean ILL ( $\bullet$ ). (C) GPP corrected for Chl <i>a</i> content to estimate photosynthetic efficiency, with a secondary axis of mean ILL ( $\bullet$ ). Letters above bars denote significant differences (X is not significantly different to any site). ....	40
Figure 3.4: Mean ( $\pm$ SE) flux of (A) ammonium (NH <sub>4</sub> <sup>+</sup> ) and (B) nitrate (NO <sub>3</sub> <sup>-</sup> ) at each site in each chamber type ( $\square$ = light chamber, $\blacksquare$ = dark chamber). Positive values indicate a production of solutes from the sediment while negative fluxes indicate a flux of solutes into the sediment. Letters above bars denote significant differences (X is not significantly different to any site). ....	42
Figure 3.5: Principle coordinate analysis (PCO) of NPP, GPP and GPP/chl <i>a</i> values with vector overlays of (A) multiple environmental variables, (B) 13 influential species indicated by simpler analyses ( <i>Aa</i> = <i>Anthopleura</i>	

*aureoradiata*, As = *Austrovenus stutchburyi*, At = *Aonides trifida*, Cl = *Colurostylis lemurum*, Hf = *Heteromastus filiformis*, Lp = *Lasaea paraengensis*, Lh = *Linucula hartvigiana*, Ml = *Macomona liliana*, Ms = *Macroclymenella stewartensis*, Md = *Magelona dakini*, Pauck = *Prionospio aucklandica*, Paust = *Paphies australis*, Th = *Torridoharpina hurleyi*) and (C) 7 functional groups indicated by simper analyses ..... 45

Figure 3.6: Principle coordinate analysis (PCO) of dark chamber fluxes of  $\text{NH}_4^+$  and  $\text{NO}_x^-$  with vector overlays of (A) multiple environmental variables, (B) 13 influential species indicated by simper analyses (codes in Figure 3.5) and (C) 7 FGs indicated by simper analyses..... 48

Figure 3.7: Mean ( $\pm$  SE) denitrification rates (production of  $\text{N}_2$ ) at sites CB and PI ( $\square$  = light chamber,  $\blacksquare$  = dark chamber)..... 55

Figure 3.8: Mean ( $\pm$  SE) nitrogen removal from the water column at sites CB and PI through ( $\square$ ) photosynthetic nitrogen uptake and ( $\blacksquare$ ) denitrification. Denitrification efficiency is displayed next to its respective column. . 56

Figure 4.1: Conceptual diagram showing nitrogen pathways at A) CB and B) PI. Thickness of lines indicates quantity of nitrogen moving through each pathway (not to scale) ..... 70

# Table of Tables

Table 2.1: Functional attributes, traits and codes for macrobenthic fauna. Source: Greenfield <i>et al.</i> , 2016.....	24
Table 2.2: Functional group number (number of species), trait code, description of trait code and example species of each functional group formed (see Appendices 1 and 2 for full species list, functional group, core and site occurrence, and abundance).....	25
Table 3.1: Mean ( $\pm$ 1 SD) Environmental and macrofauna variables reported for each site. Units specified for each variable. ....	31
Table 3.2: The 5 most abundant species sampled at each site with accompanying functional group, and individual abundance and cumulative percentage of each species. Note: CB and PI are expressed as total abundance from 20 samples, while other sites are expressed as total abundance from 10 samples.....	33
Table 3.3: PERMANOVA tests (Bray-Curtis similarity, 9999 permutations) performed on macrofauna and functional group assemblages as a function of sites. Post-hoc tests indicate all sites for both tests were significantly ( $p < 0.05$ ) different from one another. ....	36
Table 3.4: PERMANOVA tests (euclidean distance, 9999 permutations) performed on solute fluxes as a function of site. Flux data normalised before analysis. Significant effects ( $p < 0.05$ ) shown in bold. Post-Hoc pair-wise tests indicate only significant differences between sites. ....	43
Table 3.5: Two-way PERMANOVA tests (euclidean distance, 9999 permutations) performed on DIN fluxes as a function of chamber type (light and dark) by site. Flux data normalised before analysis. Significant effects ( $p < 0.05$ ) shown in bold. Post-Hoc pair-wise tests indicate only significant differences between sites. ....	44
Table 3.6: Distance based linear model (DistLM) results for the response variables of 1) dark O <sub>2</sub> (SOC), 2) dark NH <sub>4</sub> <sup>+</sup> and 3) dark NO <sub>x</sub> <sup>-</sup> flux values from 40 chambers. The full model contained 13 predictor variables: Mud content (%), organic content (OC), Chl <i>a</i> biomass, phaeophytin biomass, number of taxa, number of individuals, abundance of the functional groups BFKO, BEKN, BFMOTW, CEI, CFLO, CFQ and DJN. Values were standardised prior to analysis. ....	50
Table 3.7: Subsequent distLM models run to compare the contribution from the functional group BFKO and its constituent species ( <i>L. hartvigiana</i> , <i>L. parengaensis</i> , <i>A. bifurca</i> ) to the response variable of dark chamber O <sub>2</sub> flux.....	51
Table 3.8: Diagnostic statistics of the best fit model to predict SOC using the study variables .....	52
Table 3.9: Subsequent distLM models run to compare the contribution from the FG BFKO and its constituent species ( <i>L. hartvigiana</i> , <i>L. parengaensis</i> , <i>A. bifurca</i> ) to the response variable of dark chamber NH <sub>4</sub> <sup>+</sup> flux. ....	53

Table 3.10: Subsequent distLM models run to compare the contribution from the FG BFMOTW and its constituent species ( <i>M. liliانا</i> , <i>C. ovata</i> .) to the response variable of dark chamber NO <sub>x</sub> <sup>-</sup> flux.....	54
Table 3.11: Diagnostic statistics for the best fit model to predict NO <sub>x</sub> <sup>-</sup> using the study variables. ....	54
Table 3.12: PERMANOVA results (euclidean distance, 9999 permutations) performed on DN fluxes as a function of chamber type (light or dark) by site. Flux data normalised prior to analysis. Significant (p < 0.05) results are indicated in bold. Post-hoc pair-wise tests indicate only significant differences. ....	55

# 1. Introduction

---

New Zealand has a diverse and complex coastal geomorphology, resulting in a wide range of coastal environments (Hume *et al.*, 1992; Hume & Herdendorf, 1993; Kennedy & Dickson, 2007) including over 400 estuaries (Thrush *et al.*, 2013). New Zealand contains a range of estuaries, from coastal plains formed by flooded and expanding river valleys, deep fjords formed by glacial activity and shallow, barrier-enclosed coastal lagoons (Hesp *et al.*, 1999; Valle-Levinson, 2011; Thrush *et al.*, 2013; Badesab *et al.*, 2017). The two largest estuaries in New Zealand are the Manukau and Kaipara Harbours (drowned river valleys) (Hume & Herdendorf, 1988), situated on the west coast of the North Island, near Auckland, the country's largest city.

Estuaries are dynamic and diverse ecosystems, not only in geomorphology, but also in terms of the biological, physical and chemical processes that occur in these environments. They are among the world's most productive ecosystems (Hopkinson *et al.*, 1999; Griffiths *et al.*, 2017) and are key areas for exchanges of matter and energy, mixing inputs from terrestrial and freshwater sources with oceanic waters from the ocean (Cameron & Pritchard, 1963; Hesp *et al.*, 1999; Valle-Levinson, 2011; Thrush *et al.*, 2013). Particles and solutes are also exchanged across the sediment-water interface, altering chemical concentrations in both the water column and the benthos, which serves as an important repository for organic and inorganic matter (Hopkinson *et al.*, 1999).

The plant productivity in estuaries comes from several sources, such as the phytoplankton in the water column (e.g. Boyer *et al.*, 1993; Hopkinson *et al.*, 1999), estuarine vegetation including mangroves and seagrass (e.g. Moncrieff *et*

*al.*, 1992; Duarte & Chiscano, 1999; Gladstone-Gallagher *et al.*, 2016), macroalgae (e.g. Teichberg *et al.*, 2010; Green & Fong, 2015) and the microphytobenthos (e.g. Ní Longphuirt *et al.*, 2009; Komorita *et al.*, 2012). Estuaries are capable of high levels of productivity due to a combination of factors including; the shallow nature of many estuaries allowing light penetration to the sediments in turn stimulating photosynthesis (Ní Longphuirt *et al.*, 2009); the high levels of nutrients introduced into estuaries from terrestrial sources (Herbert, 1999) that support primary producer population growth; and the high residence times/low flushing rates of estuarine waters that retain dissolved inorganic nutrients and phytoplankton, further facilitating primary production (Heath, 1976; Perez *et al.*, 2011). These primary producers also serve as a source of organic detritus, which is deposited onto the sediment surface and remineralised into dissolved inorganic nitrogen (DIN) (Herbert, 1999), making it available for primary producers.

Shallow intertidal estuaries such as the Manukau Harbour often have prolific growth of microphytobenthos (MPB) on the sediment surface, which has been identified as both an important primary producer due to the photosynthetically active radiation reaching the sediments (Ní Longphuirt *et al.*, 2009), and as an important food source for secondary producers, including macroinfaunal suspension and deposit feeders (Needham *et al.*, 2011; Pratt *et al.*, 2015; Jones *et al.*, 2017). In intertidal habitats MPB productivity is higher than phytoplankton rates due to the prolonged exposure to high levels of photosynthetically active radiation (Varela & Penas, 1985), the steady supply of nutrients from the sediment (Herbert, 1999), and because phytoplankton is removed from the area during low tide (Joint, 1978; Varela & Penas, 1985). MPB has also been shown to play a key role in the remineralisation pathways and nutrient fluxes in coastal waters

(Hochard *et al.*, 2010), as well as serving as an important sink for removing excess nutrients (Sakamaki *et al.*, 2006; Komorita *et al.*, 2012). Additionally, increased MPB biomass has been found to have a disproportionately positive effect on the abundance of denitrifying bacteria in the sediments, in some cases by a factor of 10, resulting in higher rates of nitrogen removal from aquatic systems (Decleyre *et al.*, 2015). These bacteria reduce nitrate in anaerobic respiration, producing inert dinitrogen gas ( $N_2$ ) as an end-product (Herbert, 1999), which is then lost from the system into the atmosphere.

Estuaries provide a range of key ecosystem services that benefit humans (Griffiths *et al.*, 2017; O'Meara *et al.*, 2017) such as supporting fisheries (Houde & Rutherford, 1993; Jackson *et al.*, 2001; Marsden & Adkins, 2009) and serving as culturally and recreationally important areas (Marsden & Adkins, 2009; Bremer & Funtowicz, 2015). These ecosystems are under pressure from human activities on both land and in the water, such as nutrient and pollutant loading into harbours (Vitousek *et al.*, 1997; Syvitski *et al.*, 2005; Barbier *et al.*, 2011), overexploitation of fisheries (Jackson *et al.*, 2001), and habitat destruction/modification/fragmentation (Lotze *et al.*, 2006; see Thrush *et al.*, 2008). These anthropogenic pressures can damage estuarine ecosystems, resulting in biodiversity loss and a decrease in water quality and ecosystem functioning (Cloern *et al.*, 2015; Alberti *et al.*, 2017, Griffiths *et al.*, 2017). Nutrient supply, balance and cycling are all important processes for estuarine ecosystem health (Dollar *et al.*, 1991; Komorita *et al.*, 2012; Berelson *et al.*, 2013) and in supporting primary productivity in coastal and estuarine systems (Hopkinsons *et al.*, 1999; Komorita *et al.*, 2012).

Estuarine nutrient concentrations and dynamics are affected by freshwater inputs running off catchments (Nilsson & Jansson, 2002; Teichberg *et al.*, 2010; Decleyre *et al.*, 2015), groundwater seepage (Johannes & Hearn, 1985; Ji *et al.*, 2013), atmospheric deposition (Wild-Allen & Andrewartha, 2016), and from anthropogenic point sources such as sewage and wastewater discharges (Vitousek *et al.*, 1997; Kelly, 2008; Greenfield *et al.*, 2013; Cloern *et al.*, 2015). Land use, such as agricultural and urban development, in coastal catchments can influence the trophic status of estuaries. One such stressor from land intensification is excessive nutrient loading in coastal and estuarine waters (Vitousek *et al.*, 1997; Nilsson & Jansson, 2002; Teichberg *et al.*, 2010), which can result in large, harmful algal blooms (Decleyre *et al.*, 2015), macroalgal (marine seaweed) blooms (Teichberg *et al.*, 2010), anoxia in bottom waters (Griffiths *et al.*, 2017) and decreases in biodiversity and biomass (Gray, 1997; Haughtier *et al.*, 2009). Known as eutrophication, these impacts all influence the ecosystems ability to process and cycle these nutrients through removal and remineralisation of organic material (Hochard *et al.*, 2010; Fanjul *et al.*, 2011).

Remineralisation of nutrients occurs within the sediments as organic matter is broken down and decomposed by the microbial community (Herbert, 1999; Hopkinson *et al.*, 1999). As organic matter is deposited and builds up in the sediments, it is transformed through several steps from particulate organic matter (POM) into bioavailable dissolved inorganic nitrogen, a key process for fuelling primary production as nitrogen (as opposed to phosphorus or other trace nutrients) is often limiting in New Zealand coastal systems (Hanisak, 1983; Fry *et al.*, 2011). The source, quality (i.e. labile or refractory), quantity and spatial distribution of organic matter in the sediment affects the speed of decomposition,



and can alter the rates of ammonification, nitrification and denitrification of nitrogenous compounds (Val Klump & Martens, 1987; Herbert, 1999; Gladstone-Gallagher *et al.*, 2016). Remineralisation of organic matter occurs through a series of reduction-oxidation steps, where each form of nitrogen is chemically altered. The first transformation is ammonification (remineralisation), where organic matter is remineralised into ammonium ( $\text{NH}_4^+$ ) by heterotrophic microorganisms. In the presence of oxygen,  $\text{NH}_4^+$  is first oxidised to nitrite, which is in turn oxidised to nitrate ( $\text{NO}_3^-$ ) by ammonia and nitrite oxidising bacteria respectively. Denitrification is carried out by heterotrophic microorganisms in anaerobic conditions where no oxygen is available for respiration. This process occurs simultaneously with nitrification in a coupled process, where nitrate is produced and advected into anoxic sediments and subsequently reduced to dinitrogen gas ( $\text{N}_2$ ) or nitrous oxide ( $\text{N}_2\text{O}$ ) (Herbert, 1999).

Denitrification is a key step in this cycle as it has been shown to be the major pathway in which excess nitrogen is removed from aquatic ecosystems (Seitzinger, 1988; Dollar *et al.*, 1991; Hamersley & Howes, 2005). This removal of excess nitrogen is becoming increasingly important as estuaries and coastal waters are being loaded with nitrogen through land intensification and other anthropogenic activities (Rönnner, 1985). Figure 1.1 shows a simplified representation of nitrogen transformation and removal from estuarine systems, where nitrogen cycles between bioavailable and unavailable forms, and a simplified diagram indicating where each process occurs, the sources and sinks of nitrogen species, and the coupling of oxic-anoxic processes.

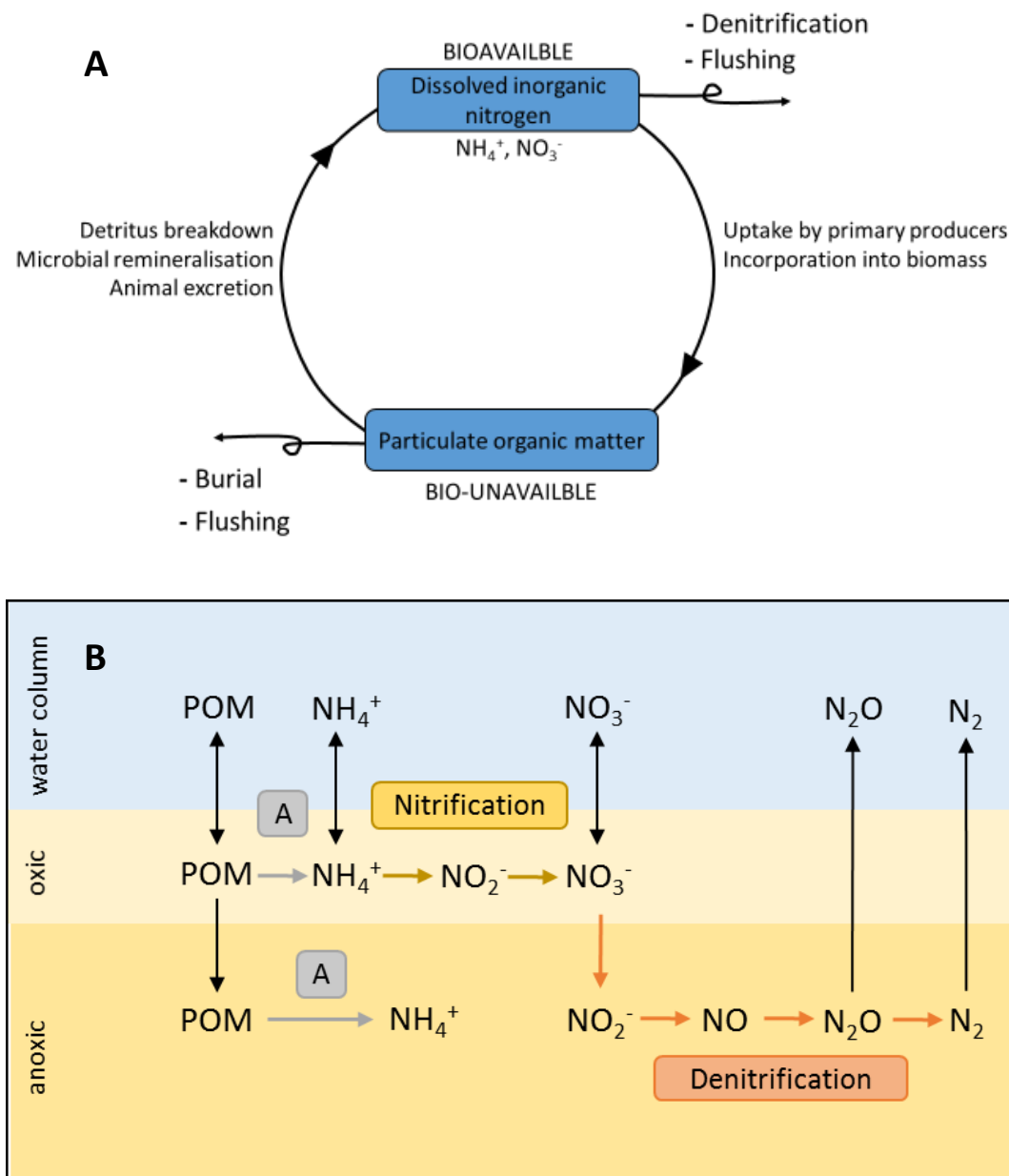


**Figure 1.1: A) Simplified diagram showing cycling of nitrogen and removal of nitrogen in benthic-pelagic coupling and B) Graphic representation of nitrogen cycling in the water column, oxic and anoxic sediments.**

As stated above, the coupling of nitrification and denitrification requires movement of solutes across oxic-anoxic interfaces in the sediment (Figure 1.1), which is facilitated by movement and feeding of macrofauna (Henriksen *et al.*, 1983; Aller, 1988; McCartain *et al.*, 2017). Macrofauna that construct and irrigate

tubes and burrows effectively extend the sediment-water interface, which increases the amount of oxic-anoxic interface area within the sediment column (Henriksen *et al.*, 1983; Aller, 1988). This elevates opportunities for solute advection across these boundaries, facilitating higher rates of nitrogen transformation (Henriksen *et al.*, 1983). Bioadvection of porewater through the sediments can also enhance denitrification (DN) through active movement of solutes between interstitial spaces, supplying the requisite nutrients to denitrifying bacteria (Henriksen *et al.*, 1983; Herbert, 1999; McCartain *et al.*, 2017).

Multiple environmental factors influence the rates of nutrient regeneration, including; temperature, which influences the metabolic activity of microorganisms and macrofauna, and the solubility and diffusion of solutes through sediments (Val Klump & Martens, 1987; Nowicki, 1994; Herbert, 1999); sediment properties, which control the movement of fluid and therefore solutes through interstitial spaces (Huettel *et al.*, 1998); and organic matter in the sediments, which influences levels of regenerated nutrients in the system (Val Klump & Martens, 1987). Sediment grain size influences the mechanisms and rate at which solutes move through the sediment, with muddier, cohesive sediments dominated by solute movement via molecular diffusion, a slow process driven by solute gradients (Lohse *et al.*, 1996; Huettel *et al.*, 1998), while sandier sediments with higher permeability are dominated by advective transport caused by wave action and bioturbation/irrigation (Webb and Theodor, 1968; Christensen *et al.*, 1984; Lohse *et al.*, 1996; Huettel *et al.*, 1998). Because of the difference of solute movement rates between these two sediment types, the bioturbation and irrigation carried out by macrofauna is an especially important process in muddier

sediments, as it can greatly increase an otherwise slow and limiting process in productive ecosystems (Joint, 1978; Henriksen *et al.*, 1983; Aller, 1988; Lohse *et al.*, 1996).

These environmental variables also influence the structure and composition of the macrofauna community. Anderson (2008) investigated the relationship between sediment grain size and animal abundance, where species demonstrated higher abundances at what can be assumed to be their optimal mud content. This estimated optimum mud content varied between species with a range of approximately 3% to 41% mud content, with distributions of different groups (e.g. Bivalvia, Spionidae, and Amphipoda) across the mud gradient (Anderson, 2008). Remineralised nutrients produced from organic matter decomposition are known to influence the macrofauna communities both spatially and temporally (Levinton & Stewart, 1988; Taylor *et al.*, 2010; Gladstone-Gallagher *et al.*, 2016), and support primary productivity, where studies have found that up to 75% of phytoplankton nutrient requirements are sourced from the benthos (Dollar *et al.*, 1991; Hopkinson *et al.*, 1999). While the macrofauna are controlled by both biotic and abiotic factors, their presence influences these same variables, enhancing organic matter decomposition (Kristensen *et al.*, 1992; Taylor *et al.*, 2010) and reworking (mixing and displacing) sediments (Aller, 1988; Lohrer *et al.*, 2005), further altering the environment in a dynamic feedback relationship.

The resident benthic macrofaunal community is controlled by heterogeneity in many abiotic factors. The physical and environmental factors such as water depth (immersion period) (e.g. Vincent *et al.*, 1994) and temperature (e.g. Levinton & Stewart, 1988; Espinosa & Guerra-Garcia, 2005); grain size (e.g. Whitlatch, 1981,

Anderson, 2008) and turbidity (e.g. Gunderson, 2000) influence the macrofauna community and shape their physical and behavioural traits. Factors that co-vary and interact with macrofaunal traits include oxygen levels (e.g. Hampel *et al.*, 2009), nutrient availability and turnover rate (e.g. Gammal *et al.*, 2016), organic matter content (e.g. Levinton & Stewart, 1988; Kelaher & Levinton, 2003) and salinity (e.g. Hampel *et al.*, 2009), as these factors will limit an organisms' metabolism. Complex relationships with other fauna, including predation and competition will also shape the community (Vincent *et al.*, 1994).

Benthic macrofauna are critical to ecosystem functioning (Thrush *et al.*, 2006; Jordan *et al.*, 2009; Fanjul *et al.*, 2011; Needham *et al.*, 2011), altering and enhancing the nutrient dynamics within the sediments and across the sediment-water interface (Aller, 1988; Cardinale *et al.*, 2012). The biodiversity of these ecosystems is known to be a key component of ecosystem function (Hewitt *et al.*, 2010; Strong *et al.*, 2015; Greenfield *et al.*, 2016) as greater numbers of species utilise available resources more efficiently, increasing productivity in diverse ecosystems (Tilman *et al.*, 1991; Greenfield *et al.*, 2016). Multiple species in an ecosystem can carry out the same functional role despite being taxonomically distinct (Simberloff & Dayan, 1991; Wilson, 1999; Blondel, 2003; Greenfield *et al.*, 2016). This leads to redundancy in the ecosystem that maintains functionality even if individual species are lost (Gitay *et al.*, 1996; Greenfield *et al.*, 2016) as the role they perform is still extant (Loreau *et al.*, 2001). Thus, species redundancy is an important concept in understanding the way that estuaries respond to and withstand stress and disturbances (Gitay *et al.*, 1996). However, there is evidence that one key species often dominates the effect that a certain group of species will have on the ecosystem where loss of this key species will have dire consequences

towards ecosystem function (Naeem *et al.*, 2002; Smith & Knapp, 2003; Sandwell *et al.*, 2009). Additionally, specific traits that influence ecosystem functioning may be unique to one or very few species within an ecosystem, and loss of these species can result in a severe reduction or loss an ecosystem role (Jain *et al.*, 2013; Pendleton *et al.*, 2014; Teichert *et al.*, 2017).

There is growing support for the idea that ecosystem functions are influenced by species-specific traits rather than raw species richness (Loreau *et al.*, 2001) and recently many scientists have been classifying species into ‘functional groups’ which describe the effects that taxonomically different but functionally similar species have on the surrounding environment (Chapin, 1993; Schleuter *et al.*, 2001; Diaz & Cabido, 2001; Norling *et al.*, 2007). These traits are known to influence multiple ecosystem functions such as primary productivity (Lohrer *et al.*, 2015), sediment stability (Harris *et al.*, 2015) and nutrient cycling (Norkko *et al.*, 2013). The benefit of such a classification scheme is that functional traits or groups can be used as surrogates for ecosystem processes (Butterfield & Suding, 2012; Villnäs *et al.*, 2017), and to measure similarities in spatially separated ecosystems with different species but similar/shared functional traits (e.g. inter-estuary/country/continental ecosystems) (Bremner *et al.*, 2003). However, each species still needs to be identified and described before it can be attributed functional traits and placed into a functional group.

Opinions differ as to how these groups should be formed (Wilson, 1999; Butterfield & Suding, 2012), whether the different species that share a functional trait perform the same role within the scope of ecosystem function, or whether this is assumed (Murray *et al.*, 2014). There are also questions about the different

terminologies associated with 'functional groups' (Blondel, 2003). However, several classification schemes exist, such as the classification of groups based on a series of behavioural, physical and life history patterns of species using varying degrees of detail (Rodil *et al.*, 2013; Greenfield *et al.*, 2016), using single-trait indices such as size (Norkko *et al.*, 2013), or taking a reverse approach of identifying the ecosystem function, the process which influences that function (such as bioturbation or bioirrigation), and then finding the species that carry out those processes (Woodin *et al.*, 2015). This thesis uses the functional group classification used by Greenfield *et al.*, (2016) and examines oxygen and dissolved inorganic nutrient exchange across the sediment-water interface as indicators of ecosystem function, and explores whether functional groups or individual 'key' species are better predictors of functioning.

This thesis focuses on identifying the functional groups and constituent species that act as the key drivers of ecosystem function in benthic ecosystems, with emphasis on the fluxes of oxygen ( $O_2$ ), ammonium ( $NH_4^+$ ) and nitrate ( $NO_x^-$ ). This study was undertaken as part of a larger study to develop a nitrogen model in the Manukau Harbour, New Zealand. The model will quantify the amount of nitrogen entering the harbour from both natural and anthropogenic sources, factor in the transformations of nitrogen within the sediments, including how it is removed, and use a mass balance approach to understand load limits for nitrogen entering the Manukau Harbour. This knowledge is important to understand the capacity of the system to cope with elevated nutrient inputs into the harbour through increased wastewater introduction as the population of Auckland City increases.

The specific objective of this study was to answer and investigate the following questions:

- How does nutrient processing vary spatially within the Manukau Harbour?
- Is the variation in ecosystem function better explained by biotic or abiotic variables?
- Which is better at predicting ecosystem function – Benthic macrofauna functional groups or the key species within these groups?

I used a functional group classification scheme for macrofauna based on behavioural, physical and life history traits of each species, combined with measures of solute fluxes as proxies of ecosystem functioning to gain an understanding of how these two factors are linked in the Manukau Harbour. Knowledge of how species and their functional groups influence ecosystem functioning is important due to the increasing rate at which species are being lost from our ecosystems due to anthropogenic stressors, where roles within the ecosystem are shifting from a natural to an altered state. Using the knowledge of how different species within functional groups play important roles in the ecosystem will help with management of our harbours and estuarine ecosystems, and benefit the key species and resources (fisheries/kaimoana) they support.



## 2. Methods

---

### 2.1 Study area

The Manukau harbour (37°00' S 174°40' E) is a large, natural harbour located on the western coastline of the North Island which opens into the Tasman Sea. The harbour has a tidal variation of between 1.9 m and 3.8 m and an area of approximately 365 km<sup>2</sup>. Manukau harbour is situated adjacent to and supports both Auckland city, New Zealand's largest and most populous urban centre (~1.5 million people), and a large area of agricultural farmland in the harbours approximately 895 km<sup>2</sup> catchment (Figure 2.1). As such, the Manukau receives inputs of treated wastewater and urban, industrial storm water and farm runoff. Consequently, the Manukau has had a history of poor water quality and eutrophication which has improved in the last 30 years due to better management of waterways and wastewater treatment (Kelly, 2008). The Manukau Harbour is relatively shallow, with an average depth of 6.1 m, and an intertidal area of approximately 62% (226 km<sup>2</sup>) of the total harbour area. The intertidal areas are dominated by sandy sediments, with muddy sediments in the outer reaches and side branches of the estuary. These intertidal sandbanks are the dominant habitat in the benthic ecosystem, and are considered ecologically important (Williamson *et al.*, 1992; Kelly, 2008). Sampling determined that the benthic macrofaunal community at these sites was found to be dominated numerically by the polychaete worms including *Aonides trifida*, *Heteromastus filiformis* and

*Magelona dakini*; bivalve species including *Austrovenus stutchburyi*, *Macomona liliana* and *Linucula hartvigiana*; and the anenome *Anthopleura aureoradiata*.

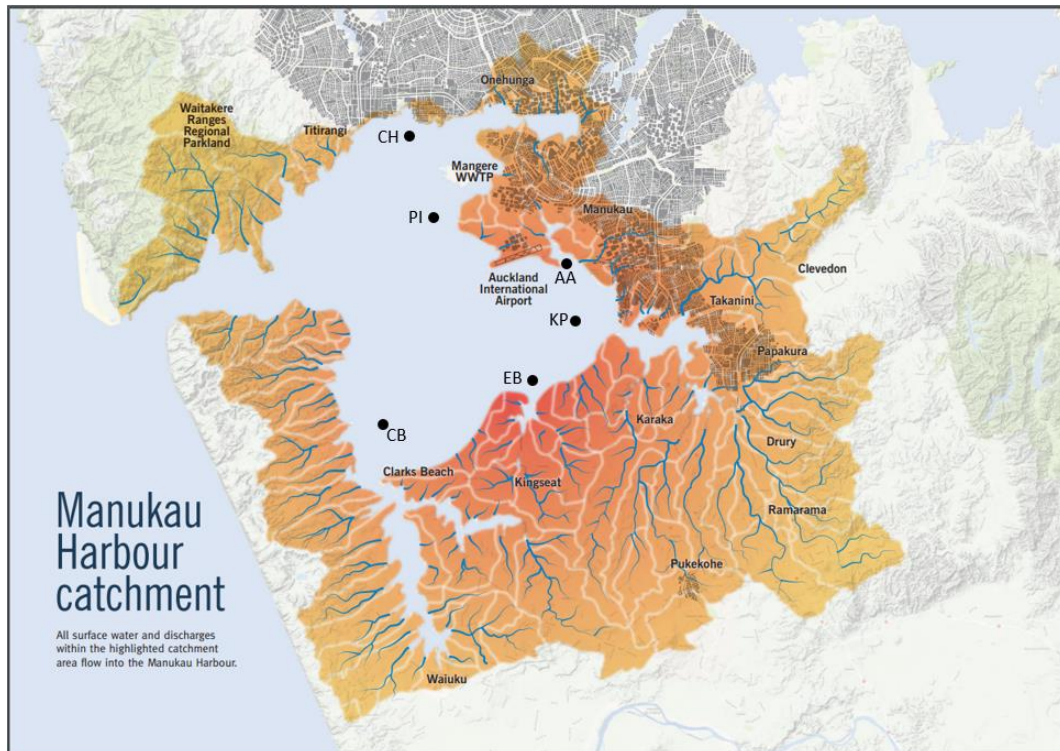


**Figure 2.1: Map of the Manukau Harbour showing the locations of study sites (CH Cape Horn, PI Pahurehure Inlet, AA Auckland Airport, KP Karaka Point, EB Elliot's Beach, and CB Clarks Beach) and the catchment area of the harbour (all water within the dark orange highlighted area flows into the harbour). Source: [www.watercare.co.nz](http://www.watercare.co.nz).**

Prior to the construction of the Mangere Wastewater Treatment Plant (MWWTP) in 1960, 675,000 L of untreated sewage and 25 million L of trade wastes were discharged into the Manukau Harbour daily (Kelly, 2008). After the construction of the MWWTP, large oxidation and sewage settling ponds were constructed within the harbour, modifying approximately 500 ha of intertidal sandflats and coastline to serve as reservoirs for these wastes. This process was continued up until the early 2000's whereupon the ponds were deconstructed and the area reopened to the rest of the harbour as part of the Wastewater 2000 Project Manukau (Figure 2.2), leading to an overall improvement in ecosystem health, however legacy nutrient impacts still exist in this area (Kelly, 2008; Fitzmaurice, 2009). Currently, the MWWTP adheres to the environmental and resource

consent guidelines laid out by the Auckland Regional Council and treats all wastewater to keep nutrient and toxin levels below acceptable thresholds, and as such ecosystem health and water quality has improved to the highest levels since the 1930's (Greenfield *et al.*, 2013; Kelly, 2014)



**Figure 2.2: A) Before and B) after the removal of oxidation settling ponds in the north-eastern area of the Manukau Harbour. Source: Iain Henderson, New Zealand Geographic.**

## 2.2 Study design

This study was performed as part of a larger project commissioned by Watercare Services Ltd. to provide information on the nutrient exchange rates and denitrification rates of the sediment for a nutrient mixing model in the Manukau Harbour. Information on the nutrient introduction into the harbour via inlets and streams was already known, however the transport of nutrients across the sediment-water interface has been shown to be an important function in coastal and estuarine ecosystems for the removal of nutrients from the water column (Barbier *et al.*, 2011, Alonso-Pérez & Castro, 2014), and as such needed to be quantified for this model.

Six study sites were chosen throughout the Manukau harbour (Figure 2.1), five of which were chosen due to their proximity to historical NIWA monitoring sites Clarks Beach (CB), Elliot's Beach (EB), Auckland Airport (AA), Cape Horn (CH) and Karaka Point (KP) to maximise linkage of the nutrient flux data produced by this experiment and historical ecological monitoring data. These sites have been monitored by NIWA due to their proximity to rivers and inlets to determine whether these inlets were negatively influencing the ecosystem quality through agricultural nutrient introduction (Greenfield *et al.*, 2013). As such there are historical records and trends of macrofauna community composition changes throughout time in response to natural and anthropogenic influences. The sixth site, PI (Pahurehure Inlet) was chosen as a point of interest due to nutrient inputs from the reopened sewage treatment ponds (Figure 2.2). The sites are all dominated by sandy (mean fine sand content of 89%), unvegetated intertidal sediments, which are considered representative of the harbour and were chosen

to provide an average nutrient turnover for the model commissioned by Watercare Services Ltd.

Flux chamber incubations were used at each of the six sites to measure nutrient changes in the water column due to benthic activity over time. The solutes analysed included dissolved oxygen (DO), ammonium ( $\text{NH}_4^+$ ), and nitrate-nitrite nitrogen ( $\text{NO}_x^-$ ). At two sites (PI and CB), additional sampling methods were employed to quantify denitrification rates through measurement of nitrogen ( $\text{N}_2$ ) flux. Sites AA, CH, EB and KP were sampled with limited replicates with five pairs of light and dark chambers, while at sites CB and PI 10 pairs of light and dark chambers were deployed. Limited replicates were deployed at the majority of sites as five chambers are adequate to provide accurate data while keeping the cost for sample processing low. Denitrification rate was only measured at two sites as the sampling is intensive and difficult, and the processing of samples is more costly than regular solute measures, however these sites were sampled with a greater number of replicates as  $\text{N}_2$  flux can be difficult to quantify and more samples are required to provide accurate data. Sediment and macrofauna cores were collected adjacent to each flux chamber for analyses.

These sites were sampled over a four-day period in December of 2016 (early summer). Flux chambers were deployed in the morning during days with high-tides near midday, and were incubated for up to 6 hours. Ambient water temperature varied between sites, however the mean temperature for all the sites during sampling was  $22.5^\circ \text{C}$ . Sites CB and PI were sampled individually over the first two days, whereas sites CH and EB, and KP and AA were sampled concurrently on days three and four (respectively).

### **2.3 In situ chamber incubations**

Each benthic chamber isolates an area of sediment (0.25 m<sup>2</sup>) and a volume of water (30 litres) above the sediment. These chambers are used to measure the production and consumption of nutrients and metabolites by the microbial community, fauna, microphytobenthos and phytoplankton, and the exchange of nutrients across the sediment-water interface. The chambers consist of an aluminium base which is pressed into the sediment to a depth of approximately 10 cm, with a removable, transparent Perspex lid which allows light penetration. Each lid has tubing installed to allow water to be removed via syringe or pump for sampling, and to allow water within the chamber to be replenished. Within each chamber a battery powered SeaBird electronics seawater pump, a D-Opto dissolved oxygen and temperature logger were attached to the chamber wall above the sediment (Figure 2.3). The seawater pump recirculated the water within the chamber (pumping for 5 seconds every 30 seconds) to prevent stagnation and localised anoxia of the isolated water.

The chambers were deployed in pairs, one light and one dark, where one chamber was covered with shade-cloth to prevent light penetration (Figure 2.3b). This method is employed to assess the production of O<sub>2</sub> in one chamber (light) through photosynthesis, while inhibiting photosynthesis in the other (dark) to measure the removal of O<sub>2</sub> through respiration of the benthic fauna and microbial communities and to restrict the nitrogen uptake by primary producers. This paired design allows for the calculation of Gross Primary Productivity (GPP) in the sediments, while the dark chamber also removes the variation of light intensity caused by changes in weather or water clarity and depth when sampling over several days and at different locations.



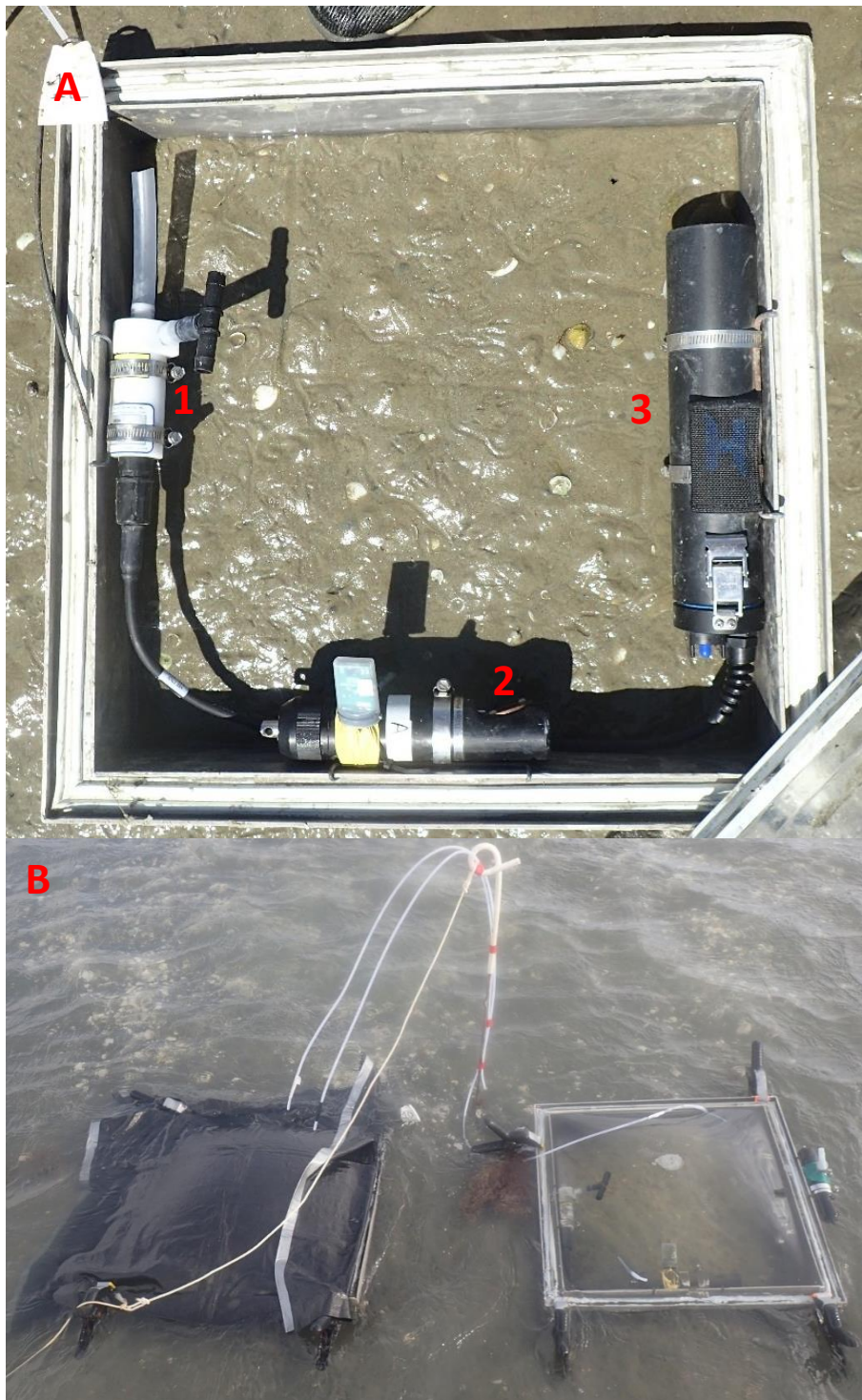


**Figure 2.3: A) The base of the flux chamber pressed into the sediment. 1) Water pump, 2) dissolved oxygen logger with HOBO data logger, 3) battery pack for water pump. B) Paired chambers with lids and shade cloth attached and sampling tubes connected after inundation. Note: DO and HOBO logger attached to the outside of the light chamber to measure the external water DO concentrations. Source: NIWA archives, 2016.**

Each chamber was deployed during low tide on an exposed sediment surface. The lids were placed on and sealed after inundation with seawater to a depth of approximately 30 cm. The chambers were left to incubate during the entire tidal

period until the water depth was approximately the same as the start of the incubation period to ensure the longest possible incubation. This method allows the calculation of changes in water chemistry through comparisons in initial and final water chemistry samples. The period between initial and final samples at these sites varied depending on tidal period and inundation depth/elevation, with incubation periods ranging from approximately 3.5 to 6 hours across these sites. Water samples for denitrification (at sites PI and CB) were collected for analyses through use of a peristaltic pump to draw water from the sealed chambers and collected in 15 ml exetainers. The pump was used to move water from the chambers into the exetainers without introducing any air bubbles which can alter N<sub>2</sub> readings during analysis. Mercuric chloride was added to the samples to prevent further microbial activity in the water sample, and capped with airtight lids to prevent atmospheric N<sub>2</sub> from interfering with the seawater N<sub>2</sub> levels. Each sample was collected in triplicate (i.e. three exetainers filled with incubated seawater from each chamber per sample). The exetainers were stored in water cooler than the ambient seawater (15 - 19° C) and then kept at 18° C in the NIWA Wellington lab until analyses using Membrane Inlet Mass Spectrometry (MIMS). The peristaltic pump was also used to fill a 60 ml syringe, which was immediately measured for dissolved oxygen (DO) (mg/L), pH and temperature using a hand held YSI ProODO Optical Dissolved Oxygen probe before filtering (Whatman GF/C glass microfiber filter, 1.2 µm pore size) into bottles for laboratory analysis. Standard water nutrient samples (without denitrification rates) were collected at sites AA, CH, EB and KP by drawing 60 ml of water from the chambers via syringe, with subsequent measurements of DO, pH and temperature were taken before filtering into bottles for laboratory analysis. These samples were kept in the dark



on ice until they could be frozen at -20° C in the NIWA Hamilton laboratory until analysis. Supplementary samples of water from the water column was conducted to quantify the ambient water variables to exclude the influence of benthic processes

## **2.4 Sampling of environmental variables**

Macrofauna samples were collected adjacent to each chamber with a 13 cm diameter core pushed into the sediment to a depth of 15 cm to quantify the composition of the benthic community at each site. Cores were sieved through a 500 µm mesh sieve and preserved in 70% Isopropyl alcohol, with 1% rose bengal later added in the lab to stain the biological material. Additionally, three sediment cores 2 cm in diameter and 2 cm depth were collected around the perimeter of the macrofauna core and amalgamated for chlorophyll *a*, grain size and organic matter content analyses.

## **2.5 Laboratory analyses**

Macrofauna samples were sorted and identified to the lowest taxonomic level practical (most often to species level), and assigned to functional groups (Table 2.1) following the method described in Greenfield *et al.*, (2016). The functional groups are determined through similarities of traits in six functional attributes which describe the species morphology, behaviour, and life history patterns. These attributes summarise the way in which the species interacts with and influences its surrounding environment.

Sediment samples were stored in the dark in a 1°C refrigerator between sampling and analysis to prevent any degradation in chlorophyll *a* (Chl *a*) or organic matter content (OC). Chl *a* analysis involved freeze drying the amalgamated sediment

samples and homogenising the sediment. A 5 g (+/- 0.01 g) subsample was taken from the freeze-dried sample and boiled in ethanol for two minutes, and then placed in the dark overnight. The next day these samples were filtered and diluted with 90% ethanol (if necessary) before being analysed with the spectrophotometer. After this initial reading, HCl acid was added to the sample to separate the degradation product (pheophytin *a*), and then reanalysed with the spectrophotometer. This method has been described in greater detail in Sartory (1982). Grain size analysis procedure involved separating the sediment samples into size fractions through standard wet sieving and pipette analyses (Poppe *et al.*, 2000). The sediment samples were initially digested with H<sub>2</sub>O<sub>2</sub> to remove OC, and washed through multiples sieves into fractions of gravel (> 2 mm), coarse sand (500 µm - 2 mm), medium sand (250 µm - 500 µm) and fine sand (63 µm - 250 µm). The remaining mud particles (< 63 µm) were then analysed by pipette analyses to determine proportions of silt and clay. OC was measured as a percentage of the total sediment weight by comparing sediment dry weight to sediment weight after removal of OC. This is achieved by drying the sample at 60°C to a constant weight (approximately 48 h) and then combusting the sample in a furnace at 600°C for 6 h. Inorganic solutes (NH<sub>4</sub><sup>+</sup> and NO<sub>x</sub><sup>-</sup>) were analysed in the NIWA Hamilton chemistry laboratory using standard methods for seawater with an Astoria-Pacific 300 series segmented flow auto-analyser with detection limits of 1 mg m<sup>-3</sup> for N.

## **2.6 Functional groups**

The use of functional groups to explore the resilience and redundancy of macrobenthic communities has been explored in previous studies (Törnroos & Bonsdorff, 2016; Greenfield *et al.*, 2016). The redundancy of species within functional groups is an important concept which states that ecosystems will

contain functionally similar species capable of performing the same function, and loss or replacement of one species will not diminish the ecosystem function significantly (Hawkins & Macmahon, 1989). For this study, the benthic macrofauna were allocated to functional groups to investigate whether individual species or the functional groups they belong to are better predictors of ecosystem functioning. The species sampled in this study were attributed to functional groups following the protocol in Greenfield *et al.*, 2016, which follows a letter allocation system based upon the traits that each species possesses (Table 2.1).

**Table 2.1: Functional attributes, traits and codes for macrobenthic fauna. Source: Greenfield *et al.*, 2016.**

Functional attribute	Functional trait	Code
Body hardness	Calcified (fully calcified shell)	B
	Soft-bodied	C
	Rigid (chitinous exoskeleton or endoskeleton)	D
Feeding behaviour	Suspension-feeder	E
	Deposit-feeder	F
	Predator/scavenger	G
	Grazer	H
Living position	Attached	I
	Above surface	J
	Top 2 cm	K
	Below surface (movement between layers)	L
	Deep	M
Movement ability	Freely mobile on or in sediment	N
	Limited movement, usually in sediment	O
	Sedentary/movement in a fixed tube	P
Living structure created	Tube	Q
	Permanent burrow	R
	Large burrow (larger crustaceans)	S
	None	T
Body size (based on adult size from Literature)	Small (< 5 mm)	U
	Medium (5 - 20 mm)	V
	Large (> 20 mm)	W

This lead to the formation of 21 functional groups containing the 80 species sampled, with 1 – 11 species in each group (Table 2.2)

**Table 2.2: Functional group number (number of species), trait code, description of trait code and example species of each functional group formed (see Appendices 1 and 2 for full species list, functional group, core and site occurrence, and abundance).**

Group (n)	Trait code	Description of traits code	Example species
1 (1)	BEI	Calcified, suspension feeding, attached	<i>Austrominius Modestus</i>
2 (2)	BEKN	Calcified, suspension feeding, top 2 cm, freely mobile	<i>Austrovenus stutchburyi</i>
3 (2)	BEKO	Calcified, suspension feeding, top 2 cm, limited mobility	<i>Diplodonta zelandica</i>
4 (1)	BEKP	Calcified, suspension feeding, top 2 cm, sedentary	<i>Arcuatula senhousia</i>
5 (7)	BF/G/HJN	Calcified, deposit feeding/predator/scavenger/grazer, above surface, freely mobile	<i>Notoacmea scapha</i>
6 (1)	BF/GKN	Calcified, deposit feeding, predator/scavenger, top 2 cm, freely mobile	<i>Turbonilla sp</i>
7 (3)	BFKO	Calcified, deposit feeding, top 2 cm, limited mobility	<i>Linucula hartvigiana</i>
8 (2)	BFMOTW	Calcified, deposit feeding, deep, limited mobility, no habitat structure, large	<i>Macomona liliana</i>
9 (1)	CEI	Soft-bodied, suspension feeding, attached	<i>Anthopleura aureoradiata</i>
10 (2)	CEQ	Soft-bodied, suspension feeding, tube structure	<i>Boccardia syrtis</i>
11 (1)	CFKN	Soft-bodied, deposit feeding, top 2 cm, freely mobile	<i>Travisia olens</i>
12 (5)	CFLN	Soft-bodied, deposit feeding, below surface, freely mobile	<i>Orbinia papillosa</i>
13 (11)	CFLO	Soft-bodied, deposit feeding, below surface, limited mobility	<i>Aonides trifida</i>
14 (7)	CFQ	Soft-bodied, deposit feeder, tube structure	<i>Macroclymenella stewartensis</i>
15 (4)	CGK/LO	Soft-bodied, predator/scavenger, top 2 cm/between layers, limited mobility	<i>Syllinae BC</i>
16 (2)	CGKN	Soft-bodied, predator/scavenger, top 2 cm, freely mobile	<i>Dorvillidae</i>
17 (9)	CGL/MNT	Soft-bodied, predator/scavenger, below surface/deep, freely mobile, no habitat structure	<i>Nemertean</i>
18 (1)	CGLPQ	Soft bodied, predator/scavenger, between layers, sedentary, tube structure	<i>Diopatra sp.</i>
19 (11)	DF/GKNT	Rigid, deposit feeding, predator/scavenger, top 2 cm, freely mobile, no habitat structure	<i>Torridoharpinia hurleyi</i>
20 (2)	DGLNS	Rigid, Predator/Scavenger, below surface, freely mobile, large burrow former	<i>Austrohelice crassa</i>
21 (5)	DJN	Rigid, above surface, freely mobile	<i>Colurostylis lemorum</i>

## 2.7 Flux calculations and data analysis

Solute fluxes were calculated by changes in water chemistry over time from initial and final sample values. The flux in each chamber was measured in  $\mu\text{mol m}^{-2} \text{h}^{-1}$  using the following equation:

$$\text{Flux} = \frac{\Delta C}{\Delta T} \times \frac{V}{A}$$

where  $\Delta C$  is the change in concentration of the solute measured ( $\mu\text{mol L}^{-1}$ ),  $\Delta T$  is the duration of incubation (hr),  $V$  is the volume of water enclosed in the chamber (L) and  $A$  is the area of isolated seafloor ( $\text{m}^2$ ) (see Macreadie *et al.*, 2006). This equation was applied to each chamber for each solute measured. Sites CB and PI displayed unexpected initial sample values in several chambers (potentially due to sampling issues with bubbles in the tubes/vials), so an average value of the initial samples was used as the initial value in all chamber flux calculations.

Denitrification rates were measured at two sites, and the denitrification efficiency of each site was calculated using the equation:

$$\text{DE} = \frac{N_2}{N_2 + \text{DIN}} \times 100$$

where  $N_2$  is the flux of nitrogen gas into the water column, and DIN is the total dissolved inorganic nutrient flux into the water column (see Macreadie *et al.*, 2006).

Further calculations to find the Gross Primary Productivity (GPP) and  $\text{GPP}_{\text{chl } a}$  were carried out by adding the amount of  $\text{O}_2$  produced in the light chamber (NPP) to the amount of  $\text{O}_2$  consumed in the paired dark chamber (SOC) to quantify the total  $\text{O}_2$  produced (GPP) by the MPB. These values were then corrected to the chl  $a$

biomass to give the  $GPP_{chl\ a}$ . Nitrogen removal rates at sites CB and PI were calculated by adding the photosynthetic nitrogen uptake rate (dark chamber - light chamber  $NH_4^+$  and dark - light  $NO_x^-$ ) to the average denitrification rates at each site. Simple histogram graphs were constructed in Microsoft Excel (2013) to visualise the mean solute fluxes at each site for each solute, with standard error bars. Multivariate PERMANOVA analyses were performed on all solute fluxes (euclidean distance) to find significant differences, and post-hoc pair-wise tests were performed on significant results to find which of these sites differed. Nitrogen fluxes ( $NH_4^+$ ,  $NO_x^-$  and  $N_2$ ) were analysed using a two-way PERMANOVA to find any site by chamber interactions.

Non-metric multidimensional scaling analyses (nMDS) were used to visualise both the multivariate raw macrofauna community data and the multivariate functional group data (note: Sample CB 10D omitted due to processing error). This data was further analysed with multivariate one-way PERMANOVA (Bray-Curtis similarity) and SIMPER analyses to determine if any differences existed between study sites, and which species and functional group were the most influential (70% cumulative contribution) to these differences. These data were not transformed prior to analysis as the difference in abundances were relatively small and transformation made no significant change in results.

Principle coordinate ordination analyses (PCO) were performed using the macrofauna and FUNCTIONAL GROUP data (Bray-Curtis similarity) to visualise the percentage of total variation between sites explained by changes in the benthic community structure. Vector overlays of predictor variables were added to determine the way in which select environmental variables influenced the

community composition between sites. Both the macrofauna/functional group data and the environmental overlays were  $\log(x+1)$  transformed prior to analyses as the environmental data was given in units of %weight and  $\mu\text{g/g}$ , which varied between predictor variables. The environmental data was also normalised prior to analyses. Multiple PCO ordinations were constructed for the multivariate solute flux data (normalised, Euclidean distance) with vector overlays of select environmental variables, influential species and influential functional groups. All PERMANOVA, MDS and PCO and associated analyses were performed with the PRIMER 7 PERMANOVA+ software.

However, the aim on the study was to determine and compare the relationship between functional groups or their constituent species and the flux of solutes into or out of the sediments. This was carried out through employing distance-based linear models (DistLM) (SAS 9.3) to identify the predictor variables most strongly associated with the solute fluxes. All predictor and response variables were standardised to values between 0 and 1 before analyses. The response variables used in the analysis were the dark chamber flux of  $\text{O}_2$ ,  $\text{NH}_4^+$  and  $\text{NO}_x^-$ , and the predictor variables chosen for primary analysis include the 7 functional groups provided by SIMPER analysis as being the most influential species, and several environmental variables known to be drivers of ecosystem functioning. Only dark chamber fluxes were analysed to remove the variable of DIN uptake via MPB and phytoplankton to focus primarily on the influence that the macrofauna have on sediment fluxes. These predictor variables were included in a model which uses backwards elimination to reject variables which are not significant at and retains variables significant at  $p < 0.15$ . The significant variables retained by this backwards SLS selection were then run through subsequent models, where



functional groups were substituted for their constituent species. The adjusted  $R^2$  values and Akaike's Information Criterion (AIC) values were used to determine whether the changes in functional group or the key species that the group contains are better predictors of ecosystem function.

## 3. Results

---

### 3.1 Environmental variables and macrofauna

Sedimentary variables were relatively similar at each study site, with a mean OC of just over 1% (range of 0.3 to 2.6%), and a mean chl *a* biomass of 9.5  $\mu\text{g g}^{-1}$  sediment (3.4 – 15.1  $\mu\text{g g}^{-1}$  sediment) (Table 3.1). The mud content shows a clear divide between the six sites, with a mean mud content of approximately 1.5%, at three sites (AA, CB, CH), and a mean mud content of approximately 9.5% at sites PI, KP and EB. Table 3.1 shows the averages and standard deviation of each of these variables at each site, however in general the sites were dominated by fine sand sediments, with low organic and mud contents. The sediment variables did not vary much within sites as each study area was intentionally placed and sampled on homogenous terrain, and the sampling area was not very large (< 20 m<sup>2</sup>). The integrated light levels (ILL) varied slightly over the four days of sampling due to a combination of weather (cloud cover), and the depth and turbidity of the water column, leading to changes in photosynthetically active radiation (PAR) reaching the chambers after inundation, as well as ambient seawater temperature. However, the weather was relatively similar over the four days of sampling. Ambient nutrient levels varied throughout the harbour, presumably due to proximity of inlets and streams which introduce these nutrients into the harbour from agricultural or urban sources. Sites CH and PI presented the highest levels of both ammonia ( $\text{NH}_4^+$ ) and nitrate ( $\text{NO}_3^-$ ) (Table 3.1), which can be attributed to their proximity to legacy nutrients from the recently removed oxidation ponds at the MWWTP (Figure 2.1).

**Table 3.1: Mean ( $\pm 1$  SD) Environmental and macrofauna variables reported for each site. Units specified for each variable.**

	AA	CH	EB	KP	CB	PI
Sand (500 - 63 $\mu\text{m}$ ) (%)	97.6 $\pm$ 2.1	99.3 $\pm$ 0.2	83.1 $\pm$ 3.2	87.1 $\pm$ 1.6	95.7 $\pm$ 1.7	87.6 $\pm$ 1.7
Mud (< 63 $\mu\text{m}$ ) (%)	1.2 $\pm$ 0.7	0.6 $\pm$ 0.1	9.1 $\pm$ 1.6	8.5 $\pm$ 0.8	2.1 $\pm$ 0.4	10.3 $\pm$ 0.7
MGS ( $\mu\text{m}$ )	133	125	129	121	127	119
Chl <i>a</i> ( $\mu\text{g g}^{-1}$ sediment)	8.6 $\pm$ 0.6	4.6 $\pm$ 0.6	11.3 $\pm$ 0.7	7.7 $\pm$ 0.3	9.5 $\pm$ 0.5	12.5 $\pm$ 1
OC (%)	0.49 $\pm$ 0.12	1.17 $\pm$ 0.08	1.13 $\pm$ 0.19	0.59 $\pm$ 0.12	0.81 $\pm$ 0.02	1.65 $\pm$ 0.29
$T_w$ ( $^{\circ}\text{C}$ )	27.1	20.6	22.6	24.0	20.4	21.3
ILL (lux)	24208 $\pm$ 5302	4245 $\pm$ 2392	23618 $\pm$ 4803	3618 $\pm$ 2555	4064 $\pm$ 1358	13535 $\pm$ 4462
Ambient $\text{NH}_4^+$ ( $\mu\text{mol L}^{-1}$ )	0.86	2.40	0.07	0.55	0.49	2.26
Ambient $\text{NO}_x^-$ ( $\mu\text{mol L}^{-1}$ )	1.19	8.05	0.23	2.90	1.15	4.67
Macrofauna abundance ( $\text{core}^{-1}$ )	102 $\pm$ 20	72 $\pm$ 13	104 $\pm$ 38	211 $\pm$ 25	89 $\pm$ 23	235 $\pm$ 43
Taxa richness ( $\text{core}^{-1}$ )	16 $\pm$ 3	11 $\pm$ 2	14 $\pm$ 3	23 $\pm$ 3	18 $\pm$ 3	18 $\pm$ 2
Taxa richness ( $\text{site}^{-1}$ )	37	23	32	50	47	45
FG richness ( $\text{site}^{-1}$ )	15	11	13	17	18	16
SWDI ( $H'$ )	2.4	1.57	1.48	2.26	2.55	2.26

*MGS* median grain size, *Chl a* Chlorophyll *a* pigment, *OC* organic content,  $T_w$  ambient water temperature at time of first sample, *ILL* average integrated light level at chamber base over incubation period, *FG* functional group, *SWDI* Shannon-Weiner diversity index.

PI and KP contained the highest abundance of macrofauna ( $211 \pm 25$  and  $235 \pm 43$  ind. core<sup>-1</sup>) and taxa ( $23 \pm 3$  and  $18 \pm 2$  sp. core<sup>-1</sup>), while CH contained the lowest macrofaunal abundance ( $72 \pm 13$  ind. core<sup>-1</sup>) and taxa richness ( $11 \pm 2$  sp. core<sup>-1</sup>, 23 sp. site<sup>-1</sup>). KP had the highest biodiversity with 50 species in total, while CB and PI presented similar high biodiversity with 47 and 45 species respectively. However, these two sites were sampled with twice the number of replicates as the other four sites so these numbers may not be consistent as rarer species are more likely to be sampled with increased sampling effort (Ellingson *et al.*, 2007; Hewitt *et al.*, 2016) (Table 3.1). Over each of the six sites a total of 80 species were identified, with a total of 11308 individual animals sampled (Appendix 1 for full species list). These sites were dominated (by abundance) primarily by the small bioturbating spionids *A. trifida* and *M. dakini*, and the capitelled *H. filiformis* (functional group CFLO) (Table 3.2) which contributed to 42% of the total animals sampled. Sites where *A. trifida* was not present (CB and CH) were dominated instead by *H. filiformis*, with either of these polychaetes making up between 26 - 69% of the animals sampled at each site. Each site was also dominated by three bioturbating bivalves, *A. stutchburyi*, *M. liliana* and *L. hartvigiana* which contributed a further 21% of the total abundance, with at least one of these bivalves present at each site (Table 3.2). Grazing surface dwelling gastropods were only present at three of the sites (EB, KP and PI), primarily the two species *Notoacmea scapha* and *Diloma subrostrata*.

**Table 3.2: The 5 most abundant species sampled at each site with accompanying functional group, and individual abundance and cumulative percentage of each species. Note: CB and PI are expressed as total abundance from 20 samples, while other sites are expressed as total abundance from 10 samples.**

Site	Species	Functional group	Abundance	Cumulative %
AA	<i>A. trifida</i>	CFLO	262	26
	<i>C. lemorum</i>	DJN	143	40
	<i>M. liliana</i>	BFMOTW	143	54
	<i>A. stutchburyi</i>	BEKN	121	66
	<i>L. parengaensis</i>	BFKO	76	73
CH	<i>H. filiformis</i>	CFLO	324	45
	<i>M. dakini</i>	CFLO	259	81
	<i>C. lemorum</i>	DJN	23	84
	<i>Aricidea spp.</i>	CFLO	12	86
	<i>M. liliana</i>	BFMOTW	12	88
EB	<i>A. trifida</i>	CFLO	725	69
	<i>A. stutchburyi</i>	BEKN	46	74
	<i>M. liliana</i>	BFMOTW	46	78
	<i>P. lyra</i>	CFLO	32	81
	<i>C. lemorum</i>	DJN	25	84
KP	<i>A. trifida</i>	CFLO	835	40
	<i>H. filiformis</i>	CFLO	281	53
	<i>M. liliana</i>	BFMOTW	203	63
	<i>M. dakini</i>	CFLO	178	71
	<i>A. stutchburyi</i>	BEKN	129	77
CB	<i>H. filiformis</i>	CFLO	484	28
	<i>A. aureoradiata</i>	CEI	253	43
	<i>L. hartvigiana</i>	BFKO	158	52
	<i>M. stewartensis</i>	CFQ	151	61
	<i>M. dakini</i>	CFLO	95	67
PI	<i>A. trifida</i>	CFLO	1593	34
	<i>A. stutchburyi</i>	BEKN	684	48
	<i>P. aucklandica</i>	CFLO	477	58
	<i>L. hartvigiana</i>	BFKO	383	67
	<i>A. aureoradiata</i>	CEI	301	73

From the species present in the study, a total of 21 functional groups were formed (see Appendix 2 for full functional group list). Of these 21 groups, 7 were present at all six sites, 7 groups contained  $\geq 5$  species, and 10 groups made up slightly more than 96% of all individuals found. CFLO was the dominant group, describing 11 species and contributing towards 56% of the total abundance (Appendix 2). This

group was present at each site, with at least two species included in the five most dominant species in five of the six sites (Table 3.2). Each of the three most abundant bivalves were grouped into three separate functional groups (BEKN, BFKO and BFMOTW) with one or two other less abundant species (Appendix 1) however despite the low biodiversity within these functional groups these groups were still some of the most abundant functional groups sampled (Table 3.2; Appendix 2).

A non-metric multidimensional scaling (nMDS) plot was constructed to visualise the difference between each site and the variation within each site based on raw macrofauna community data (Figure 3.1a). CH displayed the lowest variation with tightly grouped data points, while AA had very widely distributed data points, indicating high variation between samples. Pairwise PERMANOVA tests indicate that each site is significantly different ( $p_{\text{perm}} < 0.0001$ ) in macrofauna community composition (Figure 3.1, Table 3.3). The same plot constructed using the functional groups present in each sediment sample provide a different pattern than raw species data (Figure 3.1b). The distribution of functional group samples are less isolated from one another, showing more overlap between sites and wider variation between samples. However, multivariate PERMANOVA show that each site is still significantly different ( $p_{\text{perm}} < 0.0001$ ) from one another (Table 3.3).

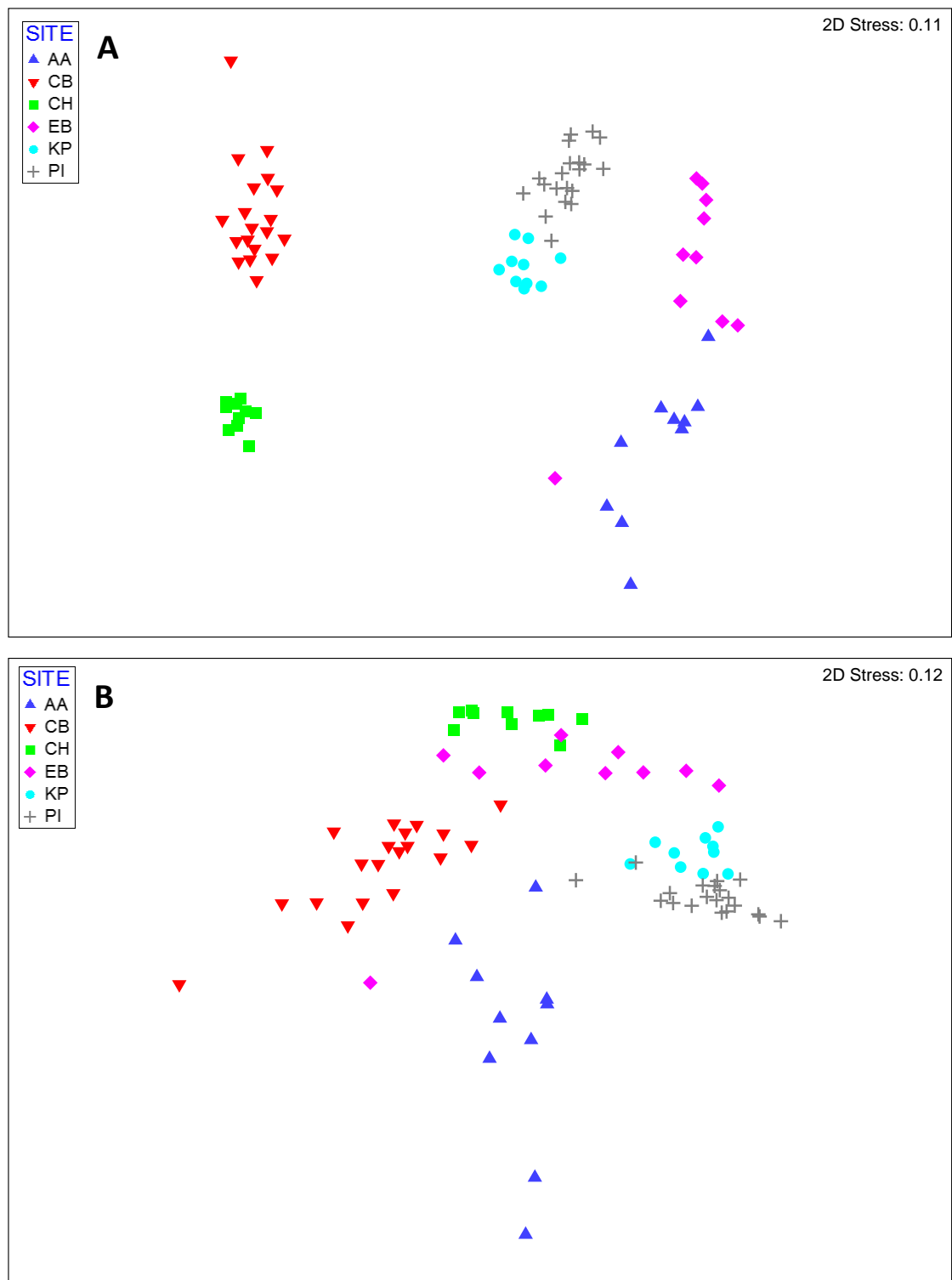


**Figure 3.1: Non-metric Multi-dimensional scaling (nMDS) (Bray-Curtis resemblance) of benthic macrofauna community composition expressed as (A) raw species data and (B) functional group abundance at each site. Each of the points on this plot indicate a single sediment core sample, and the different colours denote the six different sites**

**Table 3.3: PERMANOVA tests (Bray-Curtis similarity, 9999 permutations) performed on macrofauna and functional group assemblages as a function of sites. Post-hoc tests indicate all sites for both tests were significantly ( $p < 0.05$ ) different from one another.**

	Source	df	MS	Pseudo-F	P(perm)	Post-hoc pair-wise tests
Macrofauna	Site	5	27228	49.45	0.0001	AA≠CB≠CH≠
	Residual	74	550			EB≠KP≠PI
Functional group	Site	5	14642	36.64	0.0001	AA≠CB≠CH≠
	Residual	74	399			EB≠KP≠PI

PCO ordinations of macrofauna data and functional group data with vector overlays of select environmental variables indicate that mud, chl *a* and OC are good determining factors in the structure of macrofauna communities (Figure 3.2ab). However, they all occur along a relatively similar axis and so only explain a portion of the dissimilarities between sites, leaving a large amount of variability unexplained by these variables. This similarity in direction in which the variables influence the macrofauna and functional group data indicate they may be related to some degree. These PCO ordinations follow a similar trend as the nMDS plots, in that the functional group data are more closely related than raw macrofauna data, and show less variation.



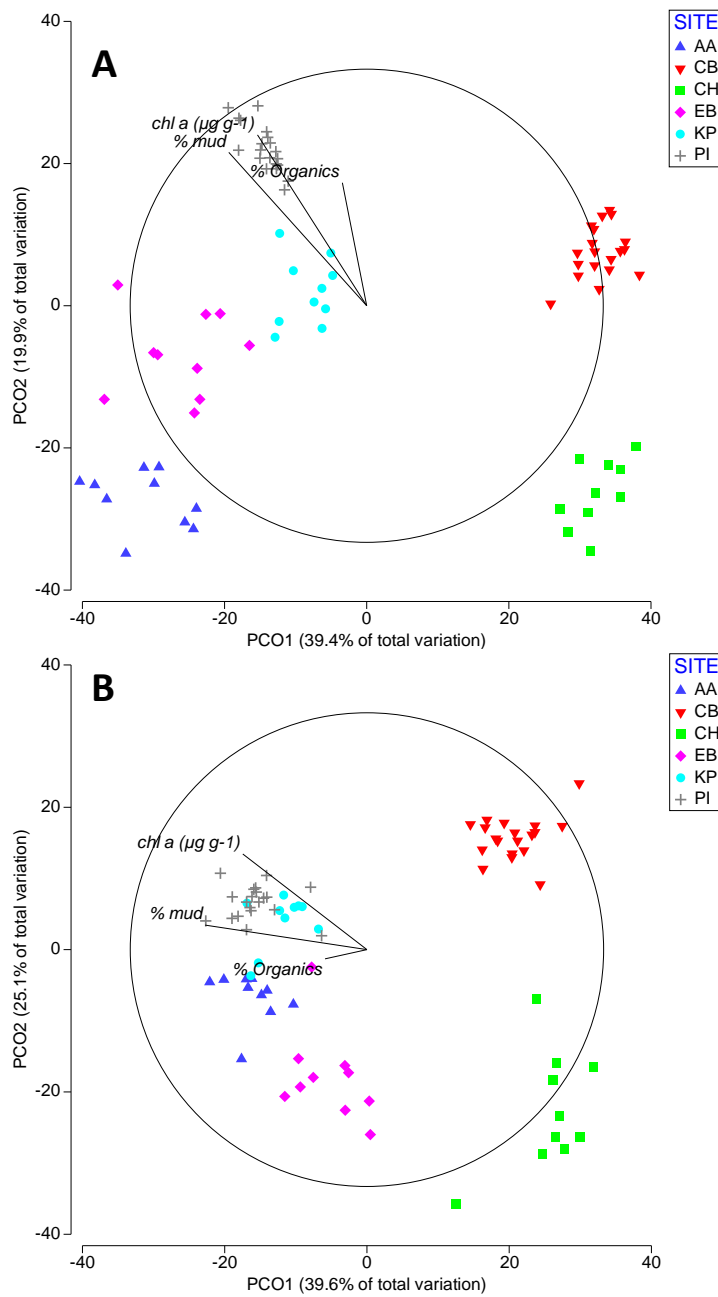


**Figure 3.2: Principle coordinate analysis (Bray-Curtis similarity) of macrofauna (Log(X+1) transformed) community expressed as (A) raw species data and (B) functional group data at each site with vector overlay of select environmental variables known to be important in structuring macrofaunal communities.**

## 3.2 Nutrient fluxes

### 3.2.1 Benthic metabolism

The oxygen flux rates over the incubation period are given in Figure 3.3, in measures of net primary productivity (NPP), sediment oxygen consumption (SOC), gross primary productivity (GPP) and GPP corrected for chl *a* content (GPP<sub>chl *a*</sub>). The dark chambers follow the expected trend of consumption (decrease) of O<sub>2</sub> during the incubation period. This consumption rate varies between sites, and this variation is very close to being statistically significant (Table 3.4,  $p_{\text{perm}} = 0.0564$ ). The flux rates in light and dark chambers are significantly ( $p_{\text{perm}} = <0.05$ ) different at four of the six sites (AA, CB, EB, PI) (Table 3.5). The SOC rates appear to correlate with the abundance of animals in the sediments (Table 3.1), with the highest of both values (abundance and consumption) at PI, and the lowest of these variables at sites CH and CB. This consumption of O<sub>2</sub> cannot be solely attributed to macrofaunal abundance however, as sites KP, AA and EB have very similar O<sub>2</sub> consumption rates, yet KP has approximately twice the mean macrofauna abundance as AA and EB (Table 3.1). The NPP at each site varied even more greatly (Table 3.4,  $p_{\text{perm}} < 0.0001$ ), with only four of the six sites demonstrating a net production of O<sub>2</sub> from the benthos. Sites CH and KP both served as a sink of O<sub>2</sub> into the sediments, despite CH having a relatively low SOC rate. These two sites had the lowest chl *a* levels in the sediment (Table 3.1), explaining why there was low O<sub>2</sub> production. Figure 3.3b and Figure 3.3c show the GPP and GPP corrected for chl *a* content respectively, while also showing the integrated light levels (ILL) measured at the chamber bases at each site. The ILL appear to fit the same trend as the GPP, with lower ILL occurring at sites with low GPP. The GPP varied greatly between sites (Table 3.4,  $P_{\text{perm}} = 0.0008$ ), ranging between  $190 \pm 69$  and  $2730 \pm$

471  $\mu\text{mol O}_2 \text{ m}^{-2} \text{ h}^{-1}$  (errors as STDERR). When corrected by chl  $a$  content, the  $\text{GPP}_{\text{chl } a}$  data follows the same trend as GPP, with a slight decrease in dissimilarity between sites (Table 3.4,  $P_{\text{perm}} = 0.0027$ ), although the differences are still statistically significant.

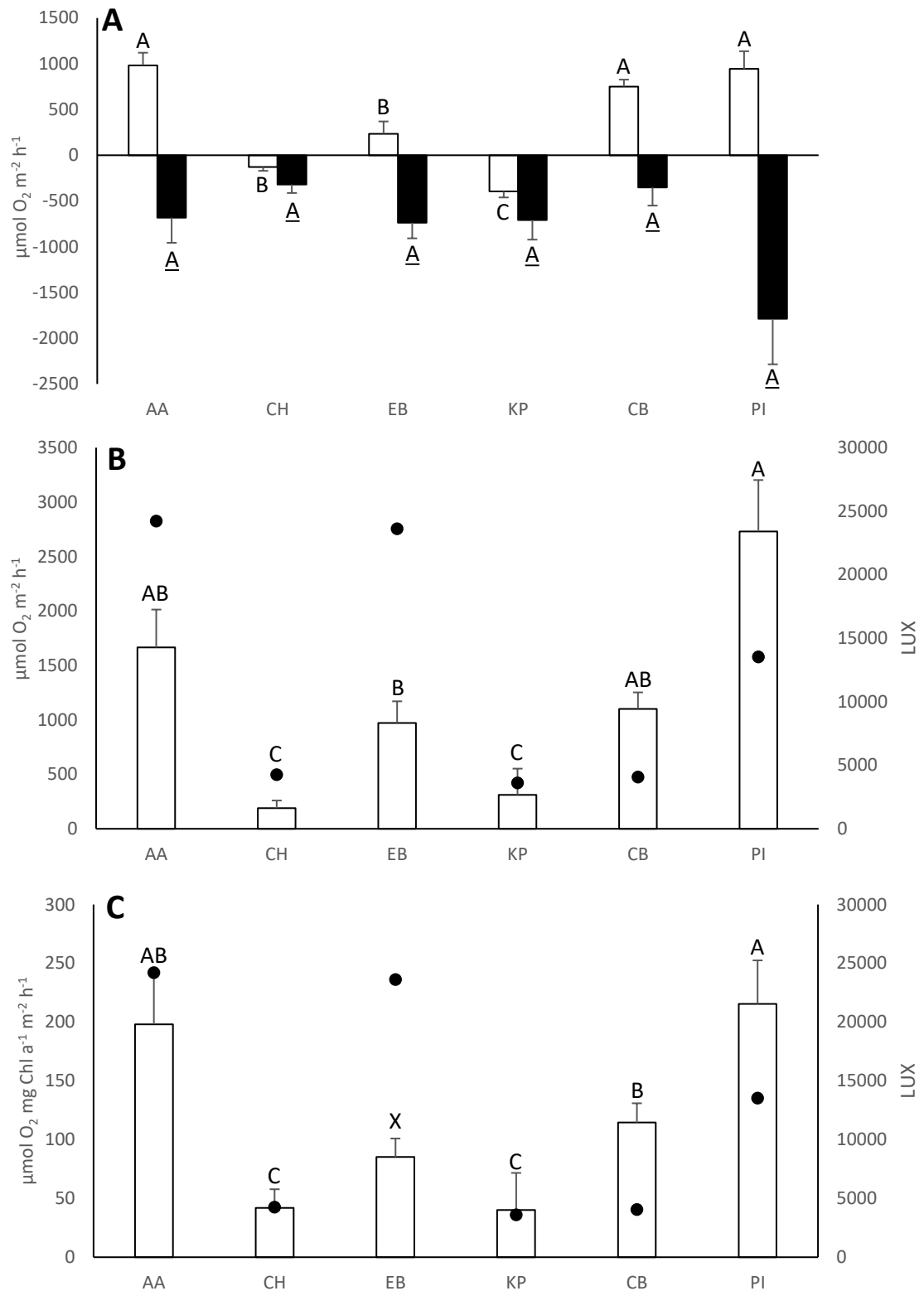


**Figure 3.3: (A)** Mean ( $\pm$  SE) dissolved O<sub>2</sub> flux at each site ( $\square$  = light chamber/NPP,  $\blacksquare$  = dark chamber/SOC). **(B)** Mean gross primary productivity at each site, with a secondary axis of mean ILL ( $\bullet$ ). **(C)** GPP corrected for Chl *a* content to estimate photosynthetic efficiency, with a secondary axis of mean ILL ( $\bullet$ ). Letters above bars denote significant differences (X is not significantly different to any site).

### 3.2.2 Nutrient regeneration

Data presented in Figure 3.4 show the mean flux rates of  $\text{NH}_4^+$  and  $\text{NO}_x^-$  for the sediments at each of the six sites in both light and dark chambers (net and gross flux respectively). These data indicate a net efflux of  $\text{NH}_4^+$ , or a movement of  $\text{NH}_4^+$  into the overlying water column, and a net influx of  $\text{NO}_3^-$ , or a movement of  $\text{NO}_x^-$  into the sediment from the water column (Figure 3.4ab). PERMANOVA tests show that while the net flux of  $\text{NH}_4^+$  does not significantly differ between sites, the gross  $\text{NH}_4^+$  flux, and both net and gross fluxes of  $\text{NO}_x^-$  are significantly different across the six sites ( $p_{\text{perm}} < 0.05$ ) (Table 3.4). PI shows the greatest variability in nitrogenous fluxes, as well as the greatest net and gross flux of  $\text{NO}_x^-$  out of the water column, with a drawdown of  $\text{NH}_4^+$  into the sediments in the light chamber, and a high rate of production of  $\text{NH}_4^+$  in the dark chambers. AA and KP seem to have similar amounts of  $\text{NH}_4^+$  being produced and  $\text{NO}_x^-$  being consumed in the sediments, while CH has an influx of both solutes. Table 3.5 gives the differences between DIN flux in light and dark chambers at each site, where only several sites (CB, EB and PI) have significantly ( $p = < 0.05$ ) lower  $\text{NH}_4^+$  fluxes in light chambers, and there is no difference in  $\text{NO}_x^-$  flux between chamber type.

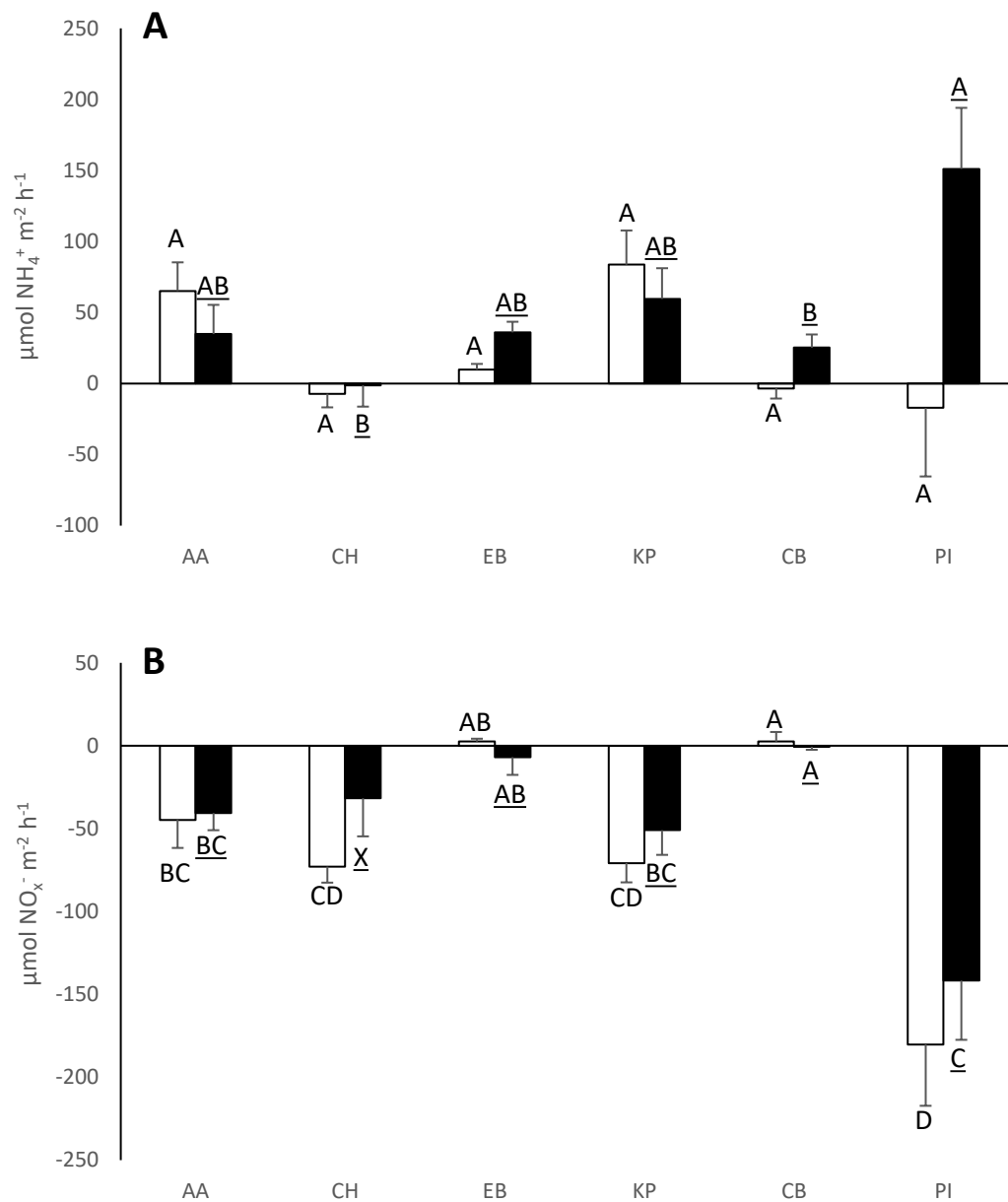


**Figure 3.4:** Mean ( $\pm$  SE) flux of (A) ammonium ( $\text{NH}_4^+$ ) and (B) nitrate ( $\text{NO}_x^-$ ) at each site in each chamber type (□ = light chamber, ■ = dark chamber). Positive values indicate a production of solutes from the sediment while negative fluxes indicate a flux of solutes into the sediment. Letters above bars denote significant differences (X is not significantly different to any site).

**Table 3.4: PERMANOVA tests (euclidean distance, 9999 permutations) performed on solute fluxes as a function of site. Flux data normalised before analysis. Significant effects ( $p < 0.05$ ) shown in bold. Post-Hoc pair-wise tests indicate only significant differences between sites.**

Ecosystem function variable	Source	df	MS	Pseudo-F	P(perm)	Post-hoc pair-wise tests
SOC	Site	5	2254000	2.35	0.0564	
	Residual	34	960650			
<b>NPP</b>	Site	5	2019400	12.72	<b>0.0001</b>	AA>CH, AA>EB, AA>KP, CB>CH, CB>EB, CB>KP, CH>KP, CH<PI, EB>KP, EB<PI, KP<PI
	Residual	34	158760			
<b>GPP</b>	Site	5	6095600	6.89	<b>0.0008</b>	AA>CH, AA>KP, CB>CH, CB>KP, CH<EB, CH<PI, EB<PI, KP<PI
	Residual	34	884930			
<b>GPP<sub>chl a</sub></b>	Site	5	36488	4.95	<b>0.0027</b>	AA>CH, AA>KP, CB>CH, CB>KP, CB<PI, CH<PI, KP<PI
	Residual	34	7373			
Net $\text{NH}_4^+$	Site	5	10475	1.34	0.2655	
	Residual	34	7827			
<b>Gross <math>\text{NH}_4^+</math></b>	Site	5	23945	3.65	<b>0.0116</b>	CB<PI, CH<PI
	Residual	34	6553			
<b>Net <math>\text{NO}_x^-</math></b>	Site	5	40677	9.03	<b>0.0002</b>	AA<CB, AA>PI, CB>CH, CB>KP, CB>PI, CH<EB, EB>KP, EB>PI
	Residual	34	4505			
<b>Gross <math>\text{NO}_x^-</math></b>	Site	5	23919	5.32	<b>0.0013</b>	AA<CB, CB>KP, CB>PI, EB>PI
	Residual	34	4492			

SOC sediment oxygen consumption, NPP net primary production, GPP gross primary production, GPP<sub>chl a</sub> GPP normalised for chlorophyll *a* biomass,  $\text{NH}_4^+$  ammonium flux,  $\text{NO}_x^-$  nitrate flux, DN denitrification rate.

**Table 3.5: Two-way PERMANOVA tests (euclidean distance, 9999 permutations) performed on DIN fluxes as a function of chamber type (light and dark) by site. Flux data normalised before analysis. Significant effects ( $p < 0.05$ ) shown in bold. Post-Hoc pair-wise tests indicate only significant differences between sites.**

Ecosystem function variable	Source	df	MS	Pseudo-F	P(perm)	Post-hoc pair-wise tests
<b>O<sub>2</sub></b>	ChxSi	5	2.54	5.45	<b>0.0005</b>	AA = L>D, CB = L>D,
	Residuals	68	0.47			EB = L>D, PI = L>D
<b>NH<sub>4</sub><sup>+</sup></b>	ChxSi	5	2.42	3.00	<b>0.0149</b>	CB = L<D, EB = L<D,
	Residuals	68	0.81			PI = L<D
NO <sub>x</sub> <sup>-</sup>	ChxSi	5	0.20	0.36	0.8812	
	Residuals	68	0.56			

*O<sub>2</sub>* oxygen flux, *NH<sub>4</sub><sup>+</sup>* ammonium flux, *NO<sub>x</sub><sup>-</sup>* nitrate flux, *ChxSi* chamber by site interaction

Figure 3.5 describes some of the determining factors of primary productivity flux values (NPP, GPP, GPP<sub>chl a</sub>) by way of PCO ordinations with vector overlays of environmental data. Each site is relatively separate from one another with some overlap between samples, however a gradient can be seen across the horizontal axis which separates the sites. Pairwise testing shown in Table 3.4 indicates that most of these sites are separated due to statistically significant differences in values of NPP, GPP and GPP<sub>chl a</sub>, which can be seen in these plots. The PCO1 axis describes almost 80% of the variation between the sites, and this variation lends to the differences between sites as well as within sites. The PCO2 axis accounts for only 20% of the variation, which is almost entirely variation within sites, as the sites are separated horizontally and not vertically (in this visualisation) (Figure 3.5).



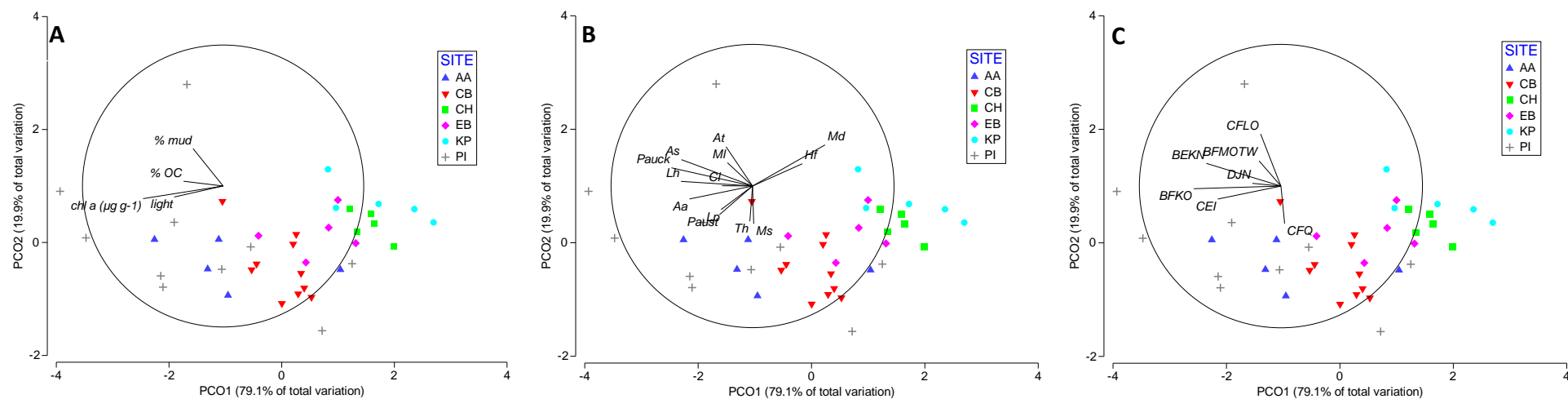


**Figure 3.5: Principle coordinate analysis (PCO) of NPP, GPP and GPP/chl *a* values with vector overlays of (A) multiple environmental variables, (B) 13 influential species indicated by simper analyses (Aa = *Anthopleura aureoradiata*, As = *Austrovenus stutchburyi*, At = *Aonides trifida*, Cl = *Colurostylis lemurum*, Hf = *Heteromastus filiformis*, Lp = *Lasaea paraengensis*, Lh = *Linucula hartvigiana*, Ml = *Macomona liliana*, Ms = *Macroclymenella stewartensis*, Md = *Magelona dakini*, Pauck = *Prionospio aucklandica*, Paust = *Paphies australis*, Th = *Torridoharpina hurleyi*) and (C) 7 functional groups indicated by simper analyses**

Figure 3.5a describes the variation in a multivariate estimate of PP by several environmental variables, with OC, chl *a* levels and light intensity explaining the horizontal component of the variation (differences between sites) while the mud content explains more of the vertical component of variability (within sites). Figure 3.5b uses vector overlays of 13 influential species (indicated as influential by SIMPER analyses), which explain variation across both axes in both directions (i.e. up and down, left and right). The abundances of the five bivalves *M. liliana*, *A. stutchburyi*, *L. parengaensis*, *P. australis* and *L. hartvigiana* point towards the left-hand side of the plot, explaining variation on both axes. Figure 3.5c uses the 7 functional groups (indicated by SIMPER analysis) to explain variation in fluxes, which appear to explain less variation than individual species. This is due to the grouping of several species into one functional group, namely the four polychaete worms in Figure 3.5b *M. dakini*, *A. trifida*, *H. filiformis* and *P. aucklandica*. While these four species point in multiple directions in Figure 3.5b, they are integrated into a single vector in Figure 3.5c, which most closely follows the path of At. The functional groups explain both horizontal and vertical variation, however horizontal variation is only explained in one direction.

Figure 3.6 shows PCO ordinations of the dark chamber fluxes of  $\text{NH}_4^-$  and  $\text{NO}_x^+$  at each of the six sites. These data show less of a gradient across the sites, with site PI demonstrating high variability between samples, while the other five sites are clustered together with much lower variability both within and between sites. This pattern is supported by the PERMANOVA analyses (Table 3.4) which indicates that the dark chamber fluxes show little significant variation between sites, with most of these significant differences occurring between site PI and others. The same variables used as vector overlays in Figure 3.5 have been used for these

ordinations, with environmental, macrofauna and functional group variables used to determine the variation in flux data. Figure 3.6a shows that the four selected environmental variables all follow a relatively similar axis, explaining variation across the PCO1 axis, however none of the selected variables explain the vertical axis, which explains about 50% of the total variation. This pattern continues in both Figure 3.6b and Figure 3.6c, where the species and functional group data explain horizontal variability in both directions, with little vertical variability explained. This indicates that there are more factors that were not sampled for which influence the nutrient regeneration in these sediments.

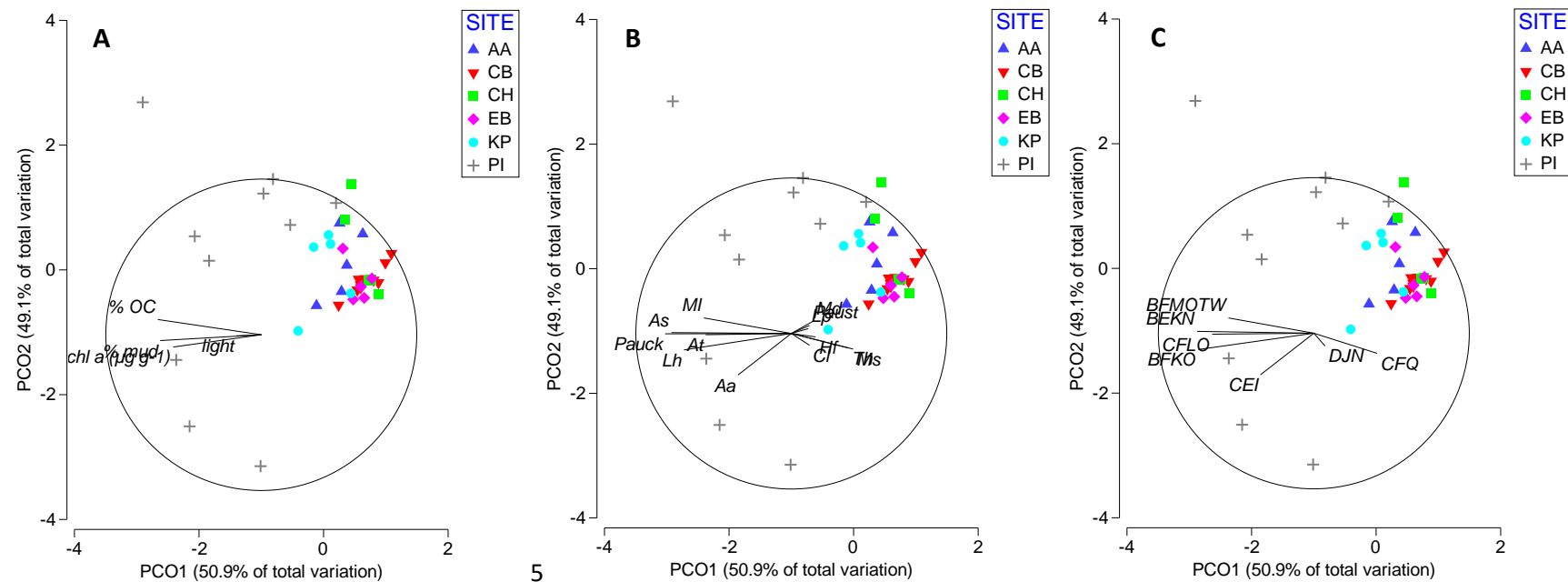


**Figure 3.6: Principle coordinate analysis (PCO) of dark chamber fluxes of  $\text{NH}_4^+$  and  $\text{NO}_x^-$  with vector overlays of (A) multiple environmental variables, (B) 13 influential species indicated by simpler analyses (codes in Figure 3.5) and (C) 7 FGs indicated by simpler analyses.**

### **3.3 Functional groups or species as predictors of ecosystem function**

Although the MDS and PCO ordination served as a visual aid to correlate solute fluxes with environmental variables, functional groups and species, these ordinations did not quantify these relationships. A distance-based linear model (DistLM) was used to quantify the best predictors of  $O_2$ ,  $NH_4^+$  and  $NO_3^-$  in dark chambers (Table 3.6), and to find whether functional groups or their constituent species served as better predictors of these fluxes (Table 3.7, Table 3.9 and Table 3.10).

Table 3.6 shows the results from three distance-based linear models which use environmental variables, macrofauna species and functional group data as predictor variables for the solute flux values (i.e. response variables). Each model produces a p value ( $Pr > F$ ) to determine the significance of the model (significance is  $<0.05$ ) and an adjusted R-square value ( $R^2$ ) which gives the strength of correlation in the model (a value closer to 1 shows a stronger correlation). The parameter estimates section indicates the relative effect strengths (positive and negative) of each significant variable, and the collinearity of each variable (VIF).

**Table 3.6: Distance based linear model (DistLM) results for the response variables of 1) dark O<sub>2</sub> (SOC), 2) dark NH<sub>4</sub><sup>+</sup> and 3) dark NO<sub>x</sub><sup>-</sup> flux values from 40 chambers. The full model contained 13 predictor variables: Mud content (%), organic content (OC), Chl *a* biomass, phaeophytin biomass, number of taxa, number of individuals, abundance of the functional groups BFKO, BEKN, BFMOTW, CEI, CFLO, CFQ and DJN. Values were standardised prior to analysis.**

<b>1) Dark chamber O<sub>2</sub></b>						
Source	DF	Sum of Squares	Mean Square	F Value	Pr > F	
Model	4	0.51468	0.12867	4.76	0.0036	
Error	35	0.94548	0.02701			
Corrected Total	39	1.46016				
Root MSE	0.16436	R-Square	0.3525			
Dependent Mean	0.67838	Adj R-sq	0.2785			
Coeff Var	24.22820					
<b>Parameter estimates based on standardised data</b>						
Variable	DF	Parameter Estimate	Standard Error	T Value	Pr >  t	Variance Inflation
Intercept	1	0.63403	0.08104	7.82	<0.0001	0
Phaeo	1	0.46240	0.20785	2.22	0.0326	3.91687
Mud	1	-0.39299	0.12380	-3.17	0.0031	2.99433
Ntaxa	1	0.27001	0.13221	2.4	0.0487	1.48745
BFKO	1	-0.34925	0.12859	-2.72	0.0102	2.31050
<b>2) Dark chamber NH<sub>4</sub><sup>+</sup></b>						
Source	DF	Sum of Squares	Mean Square	F Value	Pr > F	
Model	3	0.66107	0.22036	6.66	0.0011	
Error	36	1.19164	0.03310			
Corrected Total	39	1.85272				
Root MSE	0.18194	R-Square	0.3568			
Dependent Mean	0.28191	Adj R-sq	0.3032			
Coeff Var	64.53693					
<b>Parameter estimates based on standardised data</b>						
Variable	DF	Parameter Estimate	Standard Error	T Value	Pr >  t	Variance Inflation
Intercept	1	0.15237	0.05372	2.84	0.0074	0
Phaeo	1	-0.34735	0.22063	-1.57	0.1242	3.60177
Mud	1	0.34447	0.13089	2.63	0.0124	2.73125
BFKO	1	0.31380	0.12501	2.51	0.0167	1.78222
<b>3) Dark chamber NO<sub>x</sub><sup>-</sup></b>						
Source	DF	Sum of Squares	Mean Square	F Value	Pr > F	
Model	3	0.74599	0.24866	15.95	<0.0001	
Error	36	0.56135	0.01559			
Corrected Total	39	1.30733				
Root MSE	0.12487	R-Square	0.5706			
Dependent Mean	0.72359	Adj R-sq	0.5348			
Coeff Var	17.25715					
<b>Parameter estimates based on standardised data</b>						
Variable	DF	Parameter Estimate	Standard Error	T Value	Pr >  t	Variance Inflation
Intercept	1	0.94169	0.0064	23.17	<0.0001	0
OC	1	-0.56296	0.10160	-5.54	<0.0001	1.10795
BFMOTW	1	-0.23923	0.06277	-3.81	0.0005	1.02098
CEI	1	0.12833	0.08687	1.48	0.1483	1.12064

The final model for SOC was significant with  $p = 0.0036$ , with the predictors making the strongest contribution consisting of mud content, phaeophytin biomass,

number of taxa and the functional group BFKO ( $R^2 = 0.2785$ , AIC = -139.8) (Table 3.6). When BFKO was substituted with the abundance of its constituent species *L. hartvigiana*, it proved to be a slightly better predictor, with the total model contribution (mud, phaeo, Ntaxa, *L. hartvigiana*) giving an  $R^2 = 0.2911$  and an AIC of -140.5, though this increase is not significant (Table 3.7).

**Table 3.7: Subsequent distLM models run to compare the contribution from the functional group BFKO and its constituent species (*L. hartvigiana*, *L. parengaensis*, *A. bifurca*) to the response variable of dark chamber  $O_2$  flux.**

Dependent variable	SOC	SOC	SOC	SOC
Root mean square error	0.16436	0.16292	0.18011	0.18084
Intercept	0.63403	0.58625	0.72474	0.70934
Mud	-0.39299	-0.3972	-0.3428	-0.333
Ntaxa	0.27001	0.28208	0.10045	0.10001
Phaeo	0.46240	0.58107	0.13548	0.15115
BFKO	-0.34925	.	.	.
<i>L. hartvigiana</i> *	.	-0.4128*	.	.
<i>L. parengaensis</i>	.	.	-0.0791	.
<i>A. bifurca</i>	.	.	.	-0.0098
R-square	0.35248	0.3638*	0.22247	0.21609
Adj R-sq	0.27848	0.29109*	0.13361	0.1265
AIC	-139.797	-140.5*	-132.48	-132.15

The number of regressors in the model not including the intercept = 4, the number of parameters including the intercept = 5, the error degrees of freedom = 35. The best model is indicated by \*.

Table 3.8 shows the diagnostic statistics resultant from the best predictor variables (using *L. Hartvigiana*) for SOC put through the same distLM model. This table indicates that while the individual species serves as a slightly better predictor, the VIF of phaeophytin increases to values where it would be rejected from the model for high multicollinearity, and the differences in  $R^2$  is only marginally increased and not significantly greater.

**Table 3.8: Diagnostic statistics of the best fit model to predict SOC using the study variables**

<b>Dark chamber O<sub>2</sub></b>						
Source	DF	Sum of Squares	Mean Square	F Value	Pr > F	
Model	4	0.53121	0.1328	5	0.0027	
Error	35	0.92895	0.02654			
Corrected Total	39	1.46016				
Root MSE	0.16292	R-Square	0.3638			
Dependent Mean	0.67838	Adj R-sq	0.2911			
Coeff Var	24.01548					
<b>Parameter estimates based on standardised data</b>						
Variable	DF	Parameter Estimate	Standard Error	T Value	Pr >  t	Variance Inflation
Intercept	1	0.58625	0.087	6.74	<0.0001	0
Phaeo	1	0.58107	0.22862	2.54	0.0156	4.82306
Mud	1	-0.39715	0.12283	-3.23	0.0027	2.99973
Ntaxa	1	0.28208	0.13191	2.14	0.0395	1.5072
<i>L. hart</i>	1	-0.41276	0.14475	-2.85	0.0073	3.16716

The final model for dark NH<sub>4</sub><sup>+</sup> was significant with  $p = 0.0011$ , with the predictors making the strongest contribution consisting of phaeophytin biomass, mud content and the functional group BFKO ( $R^2 = 0.30321$ , AIC = -132.5) (Table 3.6). When BFKO was substituted with its constituent species, the results did not change and the functional group proved to be the best predictor, with the total model contribution (mud, phaeo, Ntaxa, BFKO) not changing from preliminary testing, however the difference between the first and second model (BFKO and *L. hartvigiana*) are negligible (Table 3.9).



**Table 3.9: Subsequent distLM models run to compare the contribution from the FG BFKO and its constituent species (*L. hartvigiana*, *L. parengaensis*, *A. bifurca*) to the response variable of dark chamber  $\text{NH}_4^+$  flux.**

Dependent variable	$\text{NH}_4^+$	$\text{NH}_4^+$	$\text{NH}_4^+$	$\text{NH}_4^+$
Root mean square error	0.18194	0.18198	0.19691	0.19525
Intercept	0.15237	0.18852	0.15128	0.16144
Mud	0.34447	0.34477	0.33695	0.30762
Phaeo	-0.3474	-0.4359	-0.0635	-0.0682
BFKO*	0.3138*	.	.	.
<i>L. hartvigiana</i>	.	0.35362	.	.
<i>L. parengaensis</i>	.	.	0.05351	.
<i>A. bifurca</i>	.	.	.	0.14026
R-square	0.35681*	0.35655	0.24658	0.25928
Adj R-sq	0.30321*	0.30293	0.18379	0.19755
AIC	-132.54*	-132.53	-126.21	-126.89

The number of regressors in the model not including the intercept = 3, the number of parameters including the intercept = 4, the error degrees of freedom = 36. The best model is indicated by \*.

The final model for dark  $\text{NO}_x^-$  flux produced both a stronger correlation and a different range of predictor variables than the previous response variables. The final model was significant as  $p = <0.0001$ , with the strongest contributing predictors as OC and the functional groups CEI and BFMOTW ( $R^2 = 0.57062$ , AIC = -162.65) (Table 3.6). When the functional group BFMOTW was substituted for its constituent species (CEI only contains one species), the species *M. liliana* provides the best predictor for  $\text{NO}_x^-$  fluxes, with an increase of  $R^2$  to 0.53624 and an AIC of -162.77, however this difference is negligible and not significant (Table 3.10).

**Table 3.10: Subsequent distLM models run to compare the contribution from the FG BFMOTW and its constituent species (*M. liliana*, *C. ovata*.) to the response variable of dark chamber  $\text{NO}_x^-$  flux.**

Dependent variable	$\text{NO}_x^-$	$\text{NO}_x^-$	$\text{NO}_x^-$
Root mean square error	0.18194	0.18198	0.19691
Intercept	0.15237	0.18852	0.15128
OC	-0.563	-0.5531	-0.6417
CEI	0.12833	0.12891	0.09399
BFMOTW	-0.2392	.	.
<i>M. liliana</i> *	.	-0.2467*	.
<i>C. ovata</i>	.	.	-0.1294
R-square	0.57062	0.57192*	0.4241
Adj R-sq	0.53483	0.53624*	0.3761
AIC	-162.65	-162.77*	-150.91

The number of regressors in the model not including the intercept = 3, the number of parameters including the intercept = 4, the error degrees of freedom = 36. The best model is indicated by \*.

Table 3.11 shows the diagnostic statistics resultant from the best predictor variables (using *M. liliana*) for  $\text{NO}_x^-$  put through the same distLM model. This table indicates that while the single species serves as a slightly better predictor than the functional group, the changes in parameter estimates are negligible and not significantly different.

**Table 3.11: Diagnostic statistics for the best fit model to predict  $\text{NO}_x^-$  using the study variables.**

Dark chamber $\text{NO}_x^-$						
Source	DF	Sum of Squares	Mean Square	F Value	Pr > F	
Model	3	0.74768	0.24923	16.03	<.0001	
Error	36	0.55965	0.01555			
Corrected Total	39	1.30733				
Root MSE	0.12468	R-Square	0.5719			
Dependent Mean	0.72359	Adj R-Sq	0.5362			
Coeff Var	17.23101					
Parameter estimates based on standardised data						
Variable	DF	Parameter Estimate	Standard Error	T Value	Pr >  t	Variance Inflation
Intercept	1	0.93985	0.04031	23.31	<.0001	0
org	1	-0.5531	0.1016	-5.44	<.0001	1.1112
Mac	1	-0.2467	0.06438	-3.83	0.0005	1.02665
CEI	1	0.12891	0.08675	1.49	0.146	1.12098

### 3.4 Denitrification

Site CB produced significantly ( $p_{\text{perm}} > 0.0001$ ) more  $\text{N}_2$  gas (through denitrification) than PI in both light and dark chambers (Table 3.4), and shows lower variability between samples in denitrification rate, however there is no significant difference between light and dark chambers at either site (Figure 3.7, Table 3.12).

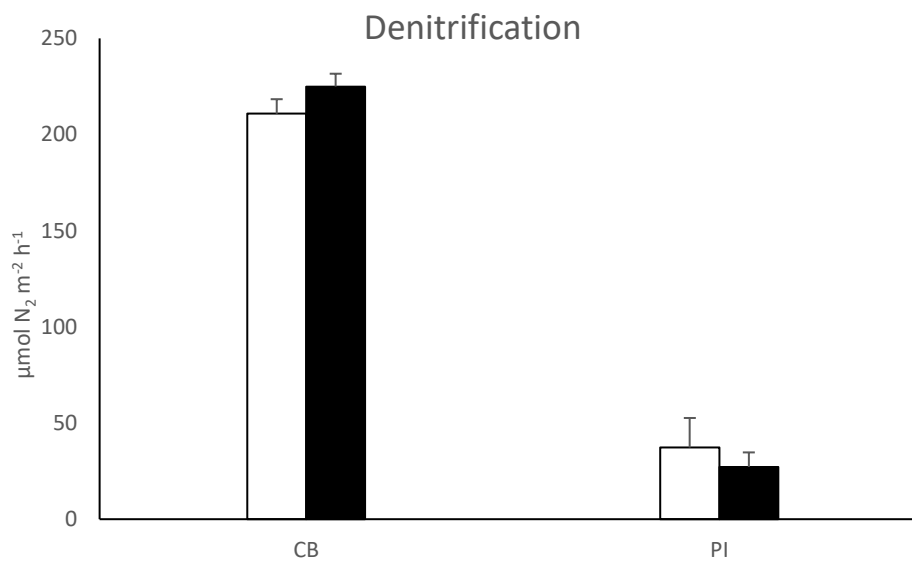


Figure 3.7: Mean ( $\pm$  SE) denitrification rates (production of  $\text{N}_2$ ) at sites CB and PI (□ = light chamber, ■ = dark chamber).

Table 3.12: PERMANOVA results (euclidean distance, 9999 permutations) performed on DN fluxes as a function of chamber type (light or dark) by site. Flux data normalised prior to analysis. Significant ( $p < 0.05$ ) results are indicated in bold. Post-hoc pair-wise tests indicate only significant differences.

Ecosystem function variable	Source	df	MS	Pseudo-F	P(perm)	Post-Hoc pair-wise tests
DN	Chamber	1	0.004	0.04	0.8463	
	<b>Site</b>	1	34.87	315.58	<b>0.0001</b>	CB>PI
	ChxSi	1	0.15	1.35	0.2536	
	Res	36	0.11			

DN denitrification rate ( $\text{N}_2$  production),

Although CB has higher rates of denitrification than PI when the total rates of nitrogen removed from the system are considered the total rates of removal are

similar ( $242.3$  and  $234.8 \mu\text{mol N m}^{-2} \text{h}^{-1}$ ), however the means of removal are different. Nitrogen removal at CB is dominated by denitrification, with almost 90% denitrification efficiency (Figure 3.8), while only a small amount of nitrogen removed through photosynthetic uptake, while PI has much higher rates of photosynthetic nitrogen removal, with only 12% denitrification efficiency. Nitrogen removal at PI is also much more variable (Figure 3.8). This shows that the majority of nitrogen is completely removed from the system at CB, while at PI the majority is fuelling primary productivity and cycling within the system.

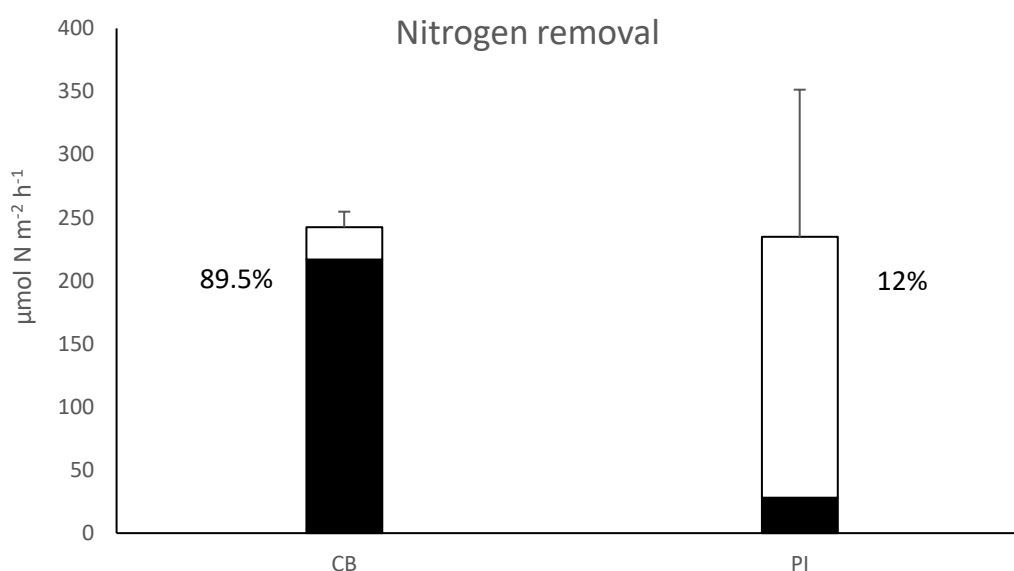


**Figure 3.8:** Mean ( $\pm$  SE) nitrogen removal from the water column at sites CB and PI through ( $\square$ ) photosynthetic nitrogen uptake and ( $\blacksquare$ ) denitrification. Denitrification efficiency is displayed next to its respective column.

## 4. Discussion

---

This study involved sampling spatially separated sites within the Manukau Harbour for measures of ecosystem functioning (solute fluxes), environmental variables and the local macrofauna community. The samples were processed and analysed with regards to relevant literature in order to understand the relationships between the variables and processes, and to answer the following questions:

- How does nutrient processing vary spatially within the Manukau Harbour?
- Is the variation in ecosystem function better explained by biotic or abiotic variables?
- Which is better at predicting ecosystem function – Benthic macrofauna functional groups or the key species within these groups?

### 4.1 Predictors of ecosystem function

In this study, I investigated whether a functional group of multiple species carrying out the same (or similar) functional roles served as a better predictor of ecosystem function than individual species from the same functional group. This was tested through multiple distLM models to find the best predictor variables for a set of response variables. Neither functional groups nor key species appeared to be better predictors of ecosystem functioning for any of the three solute fluxes tested (dark chamber  $O_2$ ,  $NH_4^+$ ,  $NO_x^-$ ) (Table 3.7, Table 3.9 and Table 3.10). For two of the response variables ( $O_2$  and  $NO_x^-$  fluxes) single species (*L. hartvigiana* (a small, deposit-feeding bivalve) and *M. Liliانا* (a large, deposit-feeding bivalve) respectively) were marginally better predictors, however, not quite statistically significant (Table 3.7 and Table 3.10). For  $NH_4^+$  fluxes the functional group BFKO

(Calcified, Deposit feeding, Top 2 cm, Limited mobility) was a better predictor than individual species were (Table 3.9). However, the improvement in adjusted  $R^2$  value in this instance (i.e. percent variability explained by the predictor) was practically negligible. Thus, the choice to use either the functional groups or the best/key single species predictors in the statistical models appears to have little practical effect on the results i.e. either choice will work equally as well.

While the distLM models do not indicate whether a functional group or its species are a better indicator of ecosystem function, they do indicate that functional groups can contain a key species that contributes substantially to the group's role in ecosystem functioning. These key species were the most numerically dominant within the functional groups that were significant in these models. Table 3.7 and Table 3.9 both show that one species has a very similar correlation to that of the functional group (e.g.  $O_2$  BFKO model  $R^2 = 0.278$ , *L. hartvigiana* model  $R^2 = 0.291$ ), while the remaining species in the functional group have very low correlations to the flux rates (e.g.  $O_2$  *L. parengaensis* model  $R^2 = 0.133$ , *A. bifurca* model  $R^2 = 0.127$ ). These results are inconsistent with the functional group redundancy concept, as, although they perform the same function, some of the species within the group do not contribute equally to ecosystem function. If these lesser species were to be lost the potential effect on the ecosystem function is likely to be minor. Conversely, if the key species (i.e. *L. hartvigiana*) were to be lost from the ecosystem or decrease in numerical dominance, there is likely to be a significant decrease in this functional group's contribution to ecosystem function (see Greenfield *et al.*, 2016). The loss or decline of key species could potentially result in the proliferation of a lesser species in the same functional group, allowing the gradual recuperation of ecosystem function. However, community recovery

dynamics are complex, determined by the extent of the disturbance, prior community, dispersal of colonists and environmental variables (Niemi *et al.*, 1990; Patrick & Swan, 2011; Woods *et al.*, 2016).

The same functional group (BFKO) and the environmental variables of mud content and phaeophytin biomass are all the best predictors for both dark O<sub>2</sub> and NH<sub>4</sub><sup>+</sup> fluxes (Table 3.7 and Table 3.9). This suggests that these two processes (community metabolism and NH<sub>4</sub><sup>+</sup> production) are linked in some way. BFKO and mud are both negatively correlated with SOC (Table 3.7), demonstrating a relationship where sites with higher abundances of these bivalve species and higher levels of mud had greater rates of O<sub>2</sub> consumption (more negative flux), consistent with other studies (Sandwell *et al.*, 2009). This increase in community metabolism is due to both the higher densities of animals increasing respiration rates, resulting in O<sub>2</sub> depletion, while also expanding the sediment-water interface, promoting exchange of solutes between the sediments and the water column (Hopkinson *et al.*, 1999; Webb & Eyre, 2004). These variables had positive relationships with NH<sub>4</sub><sup>+</sup> production, indicating that sites with an increase in BFKO abundance and mud content had higher effluxes of NH<sub>4</sub><sup>+</sup> (out of the sediment). studies have shown that bioturbation in muddy sediments facilitates NH<sub>4</sub><sup>+</sup> production and release from sediments (Webb & Eyre, 2004; Thrush *et al.*, 2006; Fanjul *et al.*, 2011), while greater macrofaunal biomass also increases NH<sub>4</sub><sup>+</sup> through excretion (Sandwell *et al.*, 2009; Lohrer *et al.*, 2016).

Flux of NO<sub>x</sub><sup>-</sup> was best correlated with the organic content (OC) and the functional groups BFMOTW (calcified, deposit feeding, deep, limited mobility, no habitat structure, large) and CEI (soft-bodied, suspension feeding, attached) (Table 3.10).

OC and BFMOTW both had negative relationships with  $\text{NO}_x^-$  flux, where sites with higher levels of organic matter and higher abundance of the functional group BFMOTW had greater  $\text{NO}_x^-$  influx (into the sediment). CEI was the opposite (greater abundance of CEI, lower flux into the sediment). Organically enriched sediments can have reduced nitrification rates due to  $\text{O}_2$  limitation in the sediments (Henriksen & Kemp, 1988). This explains the relationship between OC and  $\text{NO}_x^-$  flux, where lowered nitrification rates coupled with  $\text{NO}_x^-$  consumption by MPB and denitrifying bacteria leads to greater influx. Large bioturbating bivalves such as *M. liliانا* are known to enhance MPB biomass (Thrush *et al.*, 2004; Van Colen *et al.*, 2015) and enhance primary productivity (Woodin *et al.*, 2015), which could explain the relationship between increased  $\text{NO}_x^-$  removal and *M. liliانا* abundance as the MPB assimilates the  $\text{NO}_x^-$ . This was most evident at site PI, which had both the greatest removal of  $\text{NO}_x^-$  and the greatest GPP (Figure 3.3 and Figure 3.4). However, feeding methods carried out by *M. liliانا* drive oxygenation plumes in deeper sediments through bioadvective porewater flows (Volkenborn *et al.*, 2012; McCartain *et al.*, 2017), which would increase sediment oxygenation and facilitate more nitrification (i.e. less negative  $\text{NO}_x^-$  flux) (Woodin *et al.*, 2015). This appears to contradict to the model results in this case, uptake of nitrate by MPB likely outweighed the extra nitrification facilitated by bioirrigation.

The functional group CEI consists of only one species, *A. aureoradiata*, a small, symbiotic anemone common in New Zealand. Research has shown that these anemones harbour zooxanthellae (symbiotic dinoflagellates) which utilise dissolved inorganic nitrogen and particulate organic matter as a source of nitrogen for photosynthesis (Morar *et al.*, 2011). The relationship between CEI and  $\text{NO}_x^-$  flux suggested by the model results appears contradictory to the anemone's purported



role in the ecosystem (removing DIN), with the model results suggesting that *A. aureoradiata* either prevents  $\text{NO}_x^-$  uptake or facilitates nitrification, neither of which seem likely. However, these anemones will excrete ammonium which can facilitate nitrification. Additionally, *A. aureoradiata* is known to attach and form a mutualistic relationship with the cockle *A. stutchburyi* (Morar *et al.*, 2011), however in this study the anemone was found in high abundance at CB (253 individuals, Table 3.2), which contained only 8 cockles (Appendix 2). This indicates that the anemones were located primarily on the shell hash on the surface of the sediments, and so would be more exposed to sunlight for their photosynthesising symbionts, potentially increasing the nitrogen uptake by the anemone.

Interestingly, the functional groups which best correlated with these measures of ecosystem functioning are those with limited (BFKO and BFMOTW) to no (CEI) mobility (Table 2.2) in the sediments, indicating low bioturbation potentials, which is known to be an important factor in influencing ecosystem function (Aller, 1988; Thrush *et al.*, 2006; Jordan *et al.*, 2009; Laverock *et al.*, 2011). *A. stutchburyi* (a large deposit-feeding bivalve) was expected to have a strong relationship with ecosystem function due to previous research on the species effect on the environment (e.g. Sandwell *et al.*, 2009, Lohrer *et al.*, 2016) which show that it is an ecologically important species known to influence nutrient cycling. This was not the case here, despite the abundance of this species at several of the study sites. Additionally, the functional group CFLO and the constituent species *A. trifida* (a small, deposit-feeding polychaete) was also expected to have a similar correlation, due to the diversity of the functional group, the high abundance (Table 3.2, Appendix 2) and the bioturbation potential of the burrowing worms which is known to stimulate solute fluxes into and out of the sediment (Bartoli *et al.*, 2000).

However, these models have low  $R^2$  values ( $R^2 = 0.28$  and  $0.30$  for community metabolism and  $\text{NH}_4^+$  production respectively), indicating high unexplained variability and the potential for other contributing factors that were not assessed.

Each of the functional groups that were significant predictors of ecosystem function were low diversity groups (BFKO, BFMOTW and CEI, containing three, two and one species respectively) that were dominated numerically by a single species. This low biodiversity makes it difficult to quantify the influence the majority of species are having on ecosystem functioning. Moreover, only using the 7 functional groups indicated by SIMPER analyses leaves out the majority of groups and species that will be influencing the ecosystem functioning, whether individually or collectively.

As arranging species into functional groups is a relatively new approach (tentatively discussed in Hutchinson (1959)) and the terminologies and grouping methods are still evolving to this day (see Bengtsson, 1998; Wilson, 1999; Blondel, 2003; Schleuter *et al.*, 2010; Butterfield & Sunding, 2012; Murray *et al.*, 2014; Greenfield *et al.*, 2016), the use of functional groups is generally determined by the experiment in question. This study used a relatively fine grouping method, classifying 80 species into 21 functional groups. This method resulted in a number of groups with low species diversity and low macrofauna abundance, which were not involved in analysis as they were not contributing significantly to ecosystem functioning. This approach discounts the majority of species (the 7 functional groups included in analysis were composed of 31 species, leaving 49 species unaccounted for), despite understanding that every species will be influencing its environment in some way (Bengtsson, 1998; Blondel, 2003).

The weakness of the classification scheme and analysis used here was that it was not able to account for the entire ecosystems macrofaunal community when exploring relationships between macrofauna and ecosystem function. This has led to classification schemes designed to address specific questions or experiments, such as in Harris *et al.*, (2016), where functional groups are formed primarily around bioturbation capacity to assess the effect of macrofauna on sediment erodibility and stability. These two classification schemes contrast the two main approaches discussed in Schleuter *et al.*, (2010), where functional groups can be defined by a few behavioural or morphological characteristics, which are often easy to observe or measure, and provides coarse, easy to define groups. The second classification scheme (such as employed in this study) is defined by specific functional traits for each species. This produces a finer resolution for each group, however the traits for each species can be difficult to measure to obtain the characteristics of a whole ecosystem. Whichever classification scheme employed will have inherent limitations and benefits, however this will largely depend on how the functional groups are being analysed and what the question being addressed in the study is.

## **4.2 Solute fluxes**

Oxygen fluxes followed the predicted pattern of net photosynthetic oxygen production in light chambers (with the exception of site CH), and a net removal of oxygen in the dark chambers where photosynthesis is inhibited (Figure 3.3a). The rates of oxygen production did not correlate well with the amount of chl *a* at each site (Table 3.1). For example, EB had the second highest chl *a* biomass, but the fourth highest GPP, indicating a more complex relationship between benthic metabolism and environmental variables. Additionally, the consumption of O<sub>2</sub> is

due to the entire community of organisms present in the sediments (macrofauna, meiofauna and microorganisms), and community metabolism results appeared to match the pattern of mean number of macrofaunal individuals per site (Table 3.1). KP was an exception to this relationship, containing approximately twice the macrofaunal abundance of sites AA and EB but a very similar community metabolism to these two sites (Figure 3.3a). However, the macrofaunal data is measuring abundance, not biomass, and the meiofauna and microbes were not assessed.

When the gross primary productivity (GPP) and  $GPP_{chl\ a}$  is calculated and plotted with the integrated light levels (ILL), the variations in productivity between sites becomes clearer, with the ILL acting as a controlling factor. This is due to higher light levels allowing more efficient productivity by the MPB (AA, PI), while lower light levels reduce the productivity of primary producers (CH and KP). Fluxes at CB and EB remain anomalous, with lower GPP at EB than expected, and higher GPP at CB than expected. These contradictions to expected trends indicate that the productivity of an ecosystem is subject to multiple influences through complex feedback pathways which can be difficult to quantify. The GPP at PI may be higher than expected due to the elevated ambient nutrient levels (Table 3.1) at this site, and the higher nutrient recycling into the primary producers through photosynthetic uptake (Figure 3.8), promoting more efficient GPP. Conversely, the GPP at site EB may be lower due to the low ambient nutrient levels (Table 3.1) which may inhibit photosynthetic uptake and therefore GPP. Fluctuations in ambient  $NH_4^+$  is known to influence MPB assimilation and dynamics (Ní Longphuirt *et al.*, 2009). The GPP at PI may also be greater than expected due to high

abundance of macrofauna, which is known to increase primary productivity and nutrient cycling (Norkko *et al.*, 2013; Lohrer *et al.*, 2015).

$\text{NH}_4^+$  flux rates did not vary significantly between many sites except in the dark chambers (Table 3.4). PI had the highest flux rates of  $\text{NH}_4^+$ , consistent with expectations due to the high OC and macrofauna abundance (Table 3.1) which promotes high  $\text{NH}_4^+$  production.  $\text{NH}_4^+$  fluxes were predicted to be lower (more negative) in light chambers than in dark chambers, as  $\text{NH}_4^+$  is readily taken up by MPB during photosynthesis (Sakamaki *et al.*, 2006; Hochard *et al.*, 2010). This is true at four sites, though only three flux rates are significantly greater (Table 3.5). Two sites (AA and KP) have higher effluxes of  $\text{NH}_4^+$  in the light chamber (Figure 3.4a), contrary to predictions, however these fluxes are not significantly different between chambers (Table 3.5). These two sites have relatively low chl *a* biomass compared to other sites (Table 3.1) which will lead to less  $\text{NH}_4^+$  uptake. However, these sites both have low levels of OC, meaning less remineralisation and therefore less  $\text{NH}_4^+$  production, and greatly different macrofauna abundances, meaning different excretion rates. These unexpected fluxes may be random spikes in  $\text{NH}_4^+$  production over a short time period, and if the  $\text{NH}_4^+$  production was measured over a longer time scale this unexpected variance might not be apparent.

Figure 3.4 shows that the fluxes of  $\text{NH}_4^+$  and  $\text{NO}_x^-$  appear to be inversely related, where the greater efflux of one occurs at sites with a greater influx of the other (correlation coefficient = -0.268). The coupled ammonification-nitrification can be inferred from the efflux and influx of these solutes, where sites with high ammonium production and high nitrate consumption/removal have high rates of

ammonification, but low nitrification. Sites EB and CB have low production rates of  $\text{NH}_4^+$  and low influx of  $\text{NO}_x^-$ , which may be due to high nitrification rates, where  $\text{NH}_4^+$  is removed from the water column and converted into  $\text{NO}_x^-$ , effectively reducing  $\text{NO}_x^-$  influx. Sites with low  $\text{NH}_4^+$  production may not necessarily have low ammonification rates, but a combination of both higher nitrification rates and microphytobenthic DIN uptake. The sites with lower  $\text{NO}_x^-$  influxes (less negative) have either higher nitrification rates (production of  $\text{NO}_x^-$ ), lower  $\text{NO}_x^-$  consumption rates, high denitrification rates (only quantified at two sites) or a combination of these factors.

One of the difficulties in interpreting solute flux data is that the individual fluxes are being examined in isolation from one another, despite them occurring as coupled and complimentary processes. This can lead to inaccuracies and complications in interpreting data as it is difficult to determine how much of the solute flux is due to sedimentary processes (i.e. how much of the  $\text{NO}_x^-$  removal is due to denitrification) or how much is due to biotic interactions (i.e.  $\text{NO}_x^-$  assimilation by MPB).

### **4.3 Environmental controls of macrofauna**

Figure 3.2 shows that sediment mud and chl *a* content are both strongly correlated with benthic community structure. These factors vary spatially across the Manukau in response to hydrodynamic processes and other environmental drivers (including terrigenous sediment loading). Mud seems to be the strongest control of macrofauna distribution, with the three least muddy sites (AA, CB, CH) (Table 3.1) holding only 30.5% of the total macrofauna abundance. This result was driven largely by the abundance of a single species *A. trifida*, which contributes 3153

individuals to the muddy sites (EB, KP, and PI) (Appendix 1), making up 39.7% of these site's abundance.

All types of taxa (worms, bivalves, gastropods etc.) increased in abundance with increasing mud content except for cumaceans and isopods (crustacea), which decreased by approximately 40%. This trend followed the animal-sediment relationships laid out in Anderson (2008), where the cumacean *Colurostylis lemurum* and the amphipod *Waitangi brevirostris* preferentially live in sediments with an estimated optimum mud content of 3.4% and 7.5% respectively, while species such as *A. stutchburyi*, *L. hartvigiana* and *P. aucklandica* prefer sediments with mud contents of 11.3% to 12.2%, slightly higher than the mud content at sites EB, KP and PI. However, the decrease in rigid-bodied species is primarily due to a large abundance of *C. lemurum* at AA, while there is minor variation between other species. The species *H. filiformis* has an estimated optimum mud content of 23.4%, however in this study the abundance of this Capitellid worm decreases with increasing mud content. This can be explained by the increase in competition from other species in the same or similar functional groups, such as *A. trifida* and *P. aucklandica*, indicating that inter-species interactions are important factors in regulating community composition in addition to the environmental controls.

While the mud content of these sites is an important determining factor in structuring macrofauna communities, the mud content at the six sites ranged between 0.6 and 10.3% (Table 3.1), which is a relatively small gradient as these sites were chosen to be representative of sandy habitats. Mud content in estuaries can increase up to 92% in New Zealand (Robertson *et al.*, 2015), and the distribution and abundance of macrofauna communities varies significantly across

this gradient. As the mud gradient across the sites in this study is relatively small, the effects of such a variable are not pronounced.

Understanding how the spatial variation of environmental variables controls the benthic community is important for understanding how ecosystem functioning varies spatially, as each one of these factors influences one another in a dynamic feedback system. Altering the environment (through processes such as nutrient or sediment loading) can have cascading effects on both benthic communities and ecosystem functioning, often to the detriment of the system. This can alter solute fluxes and ecosystem functioning as the macrofauna communities and populations that regulate and influence these processes are altered, causing greater variation in ecosystem function spatially and temporally.

#### **4.4 Denitrification**

Figure 3.7 shows that CB has a significantly (Table 3.12,  $p = 0.0001$ ) higher denitrification rate than PI, producing approximately 6.8 times more  $\text{N}_2 \text{ m}^{-2} \text{ h}^{-1}$ . This is likely due to the abundance of burrowing tubeworms at CB (primarily *M. stewartensis* and other members of functional groups CEQ and CFQ) (Table 3.2, Appendix 2), which increase the oxic-anoxic interface and can facilitate coupled nitrification-denitrification (Mayer *et al.*, 1995; Svensson & Leondardson, 1996; Risgaard-Petersen, 2004). Studies have shown that burrowing animals can extend the surface area of the sediments significantly (up to a 770% increase (Webb & Eyre, 2004), Needham *et al.*, 2011), therefore increasing the area in which biogeochemical processes occur, including nitrification of  $\text{NH}_4^+$  (Pelegri *et al.*, 1994; Mayer *et al.*, 1995). Macrofauna burrows also serve as rich environments for high density bacterial colonies (Pelegri *et al.*, 1994; Webb & Eyre, 2004),



resulting in increased rates of coupled nitrification-denitrification (Henriksen & Kemp, 1988). Furthermore, the increased nitrification occurring within the burrows limits the amount of DIN assimilated by MPB on the sediment surface, so it is more freely available for denitrifying bacteria within the sediments (An & Joye, 2001).

Site PI had high primary productivity (Figure 3.3b) and higher chl *a* biomass than CB (Table 3.1), factors that are known to reduce  $\text{NH}_4^+$  and  $\text{NO}_x^-$  availability for denitrifying bacteria through direct uptake by MPB (Sundback *et al.*, 2004; Ní Longphuirt *et al.*, 2009; Hochard *et al.*, 2010). This was likely the mechanism for reduced denitrification rates at this site. This is supported by Figure 3.4a and Figure 3.4b, which show a removal of  $\text{NH}_4^+$  and  $\text{NO}_x^-$  in the light chambers at PI. Furthermore, PI hosts an abundant and diverse macrofauna community which can stimulate primary productivity of MPB (Aller, 1988; Lohrer *et al.*, 2004; Thrush *et al.*, 2006), prompting further inorganic nitrogen uptake and more  $\text{O}_2$  production. Greater  $\text{O}_2$  production by MPB leads to an increase in sediment oxygen levels, further suppressing denitrification by reducing the anoxic environment and inhibiting anaerobic bacteria (Seitzinger, 1988; An & Joye, 2001).

Examination of the total amount of DIN being removed from the sites CB and PI (photosynthetic nutrient uptake and denitrification) (Figure 3.8), suggests that competition for DIN at PI is reducing/suppressing denitrification. Both CB and PI had very similar rates of total DIN removal, however, the pathway of removal differed between sites. Nitrogen removal at CB was dominated by denitrification, with nitrogen removed permanently from the system as  $\text{N}_2$  gas, while nitrogen removal at PI was dominated by photosynthetic uptake (Figure 3.8). This

incorporation into the MPB serves as a short-term sink for nitrogen, with nutrient regeneration occurring over short temporal scales as the MPB degrades or is eaten by macrofauna. These different pathways are demonstrated in Figure 4.1.

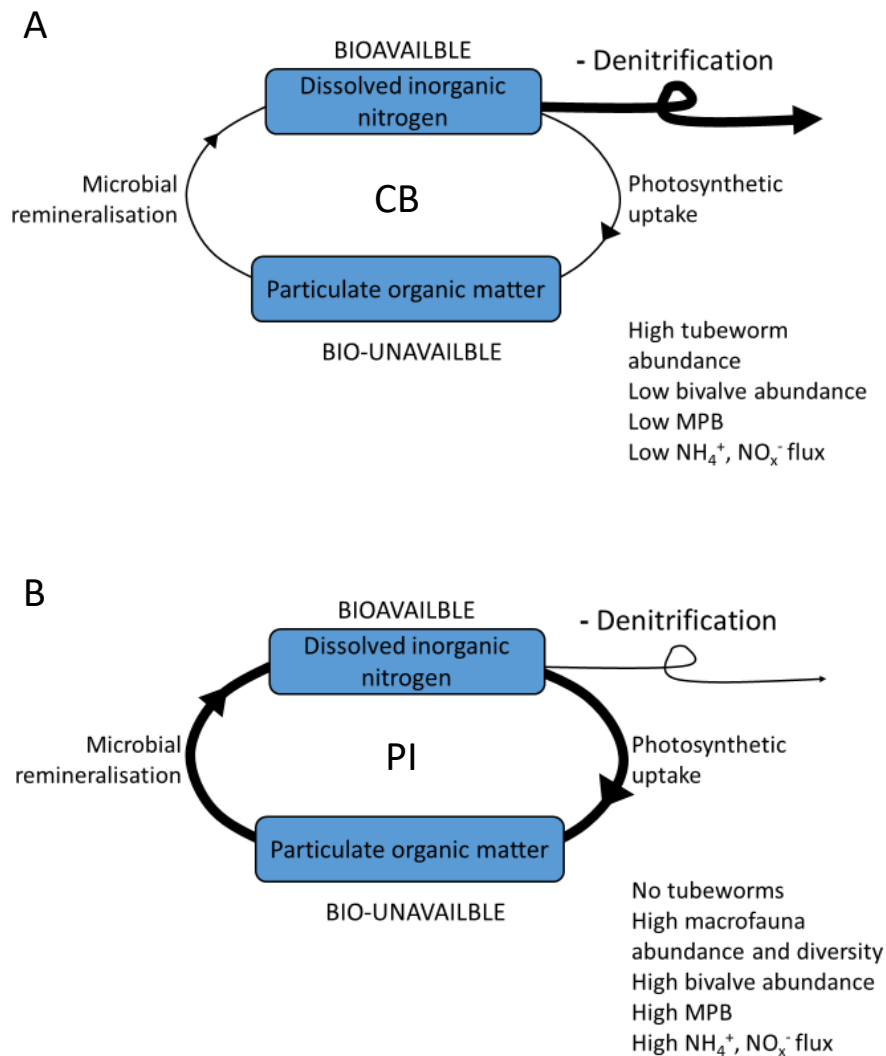


**Figure 4.1: Conceptual diagram showing nitrogen pathways at A) CB and B) PI. Thickness of lines indicates quantity of nitrogen moving through each pathway (not to scale)**

These denitrification rates provide some confounding data for a nutrient mixing and removal model in the Manukau Harbour. Extrapolation of these data will likely produce highly variable model results for the harbour, as the denitrification at these two sites appears contradictory to previous studies (Grundmanis & Murray, 1977; Henrikson & Kemp, 1988; Herbert, 1999; Sundbäck *et al.*, 2000). These

studies have shown that sandy sites often displayed higher MPB assimilation of  $\text{NO}_x^-$  than denitrification, and muddy sites often display equal or greater rates of nitrogen removal through denitrification (Sundback *et al.*, 2004 and references therein).

#### **4.5 Modelling and extrapolation**

As this data was collected in part for a nutrient mixing model in the Manukau Harbour, the rates of nutrient uptake, regeneration and removal by sediments will be extrapolated from these six sites to the whole estuary, presumably on an annual basis. The environmental variables (grain size, chl *a* and OC) had low variability between replicates and relatively low variation between sites (Table 3.1), meaning these can be extrapolated with relative accuracy, as these sites were chosen to be similar, representative habitats within the harbour. These variables also served as good predictors of the ecosystem functioning and so have the potential to be useful in scaled-up models. The macrofauna abundance is subject to greater variation than the environmental variables, with greater intra-and inter site variability, and as such is less reliable when scaled up. The solute fluxes were highly variable (Figure 3.3 and Figure 3.4), especially at site PI, and so these will be difficult to scale up accurately to model the nitrogen cycling of the entire estuary. The two denitrification rates quantified in this study were highly variable between the two sites (Figure 3.7). However, the total nitrogen removed from each of these sites through denitrification and assimilation by MPB is very similar (although highly variable at PI) (Figure 3.8), and so this can be extrapolated spatially to provide insight into the nitrogen cycling of the whole estuary for the nutrient mixing model and mass balance nutrient budget.

Calculating the annual flux of  $N_2$  gas from the sediments provides key information to ecosystem management, however the sampling and extrapolation of these flux values can lead to extremely variable denitrification rates and a poor understanding of how much nitrogen is being removed from the system. For example, the annual flux of  $N_2$  gas extrapolated over the whole harbour using data from site CB is approximately  $19,500 \text{ tonnes}^{-1} N_2 \text{ y}^{-1}$ , while using the  $N_2$  flux rate at PI gives an annual nitrogen removal of approximately  $2,900 \text{ tonnes}^{-1} N_2 \text{ y}^{-1}$ , nearly an order of magnitude lower. Using denitrification rates from single or limited number of sites thought to be representative of the harbour can produce extremely variable results, and can influence management decisions with inaccurate data.

Extrapolating to understand the annual removal of nitrogen from the systems is important for Watercare Services Ltd. as they can compare this removal rate to their annular introduction of nutrients from the MWWTP into the Manukau Harbour to ensure they are not overloading the harbour with excess nutrients.

#### **4.6 Future work**

To further increase the understanding of how macrofaunal functional groups can be used to estimate ecosystem functioning, experimental biomanipulation studies such as in Lohrer *et al.*, (2004), Norling *et al.*, (2007) and Sandwell *et al.*, (2009) can be utilised to measure the effect of the same ecosystem with one species abundance either reduced or increased. This would provide a quantifiable measure of the influence a single species or functional group has on ecosystem function while maintaining consistency among other variables. Additionally, measuring the ecosystem function and macrofauna functional groups across an

environmental gradient such as turbidity or grain size will provide important information for estimating the spatial variation in nutrient fluxes. These experiments will help in building whole-estuary nutrient mixing models such as the basis for this study, as extrapolating variable data from 6 sites across a whole estuary can lead to inaccuracies and false assumptions in the model.

Furthermore, as this study was performed in early December, this data is restricted to early summer periods, while both biotic and abiotic variables will change throughout the year with changes to the resident macrofauna community, temperature and weather patterns. Carrying out multi-year or seasonal experimentation to quantify ecosystem functioning over temporal variation is important as nutrient fluxes change seasonally in response to the aforementioned variables (Sundback *et al.*, 2000).

Additionally, the key species in each functional group are the most numerous, while the less common species in the functional groups appear to lend little influence to ecosystem functioning. This is because no weighting has been put on the functional groups role within the ecosystem, and so while the species are separated by functional groups, these functional groups are all deemed equal with regards to their effect on ecosystem functioning. As we understand that bioturbation, bioirrigation and biostabilisation are all key factors influencing nutrient pathways (Aller, 1988; Volkenborn *et al.*, 2012; Harris *et al.*, 2015), a model that adds weighting to functional groups with these attributes could provide better results.

## 5. Conclusion

---

I measured environmental variables, macrofauna community structure and fluxes of nitrogen and oxygen at six spatially separated sites within the Manukau Harbour, and analysed the way in which these factors influenced one another. Macrofauna were assigned to functional groups, and regression modelling was employed to investigate whether functional groups or species served as better predictors of ecosystem function. The findings of this study were:

- Solute fluxes vary spatially across Manukau Harbour due to their complex relationships and feedback pathways with biotic and abiotic variables.
- Functional groups and their key species serve equally as well as predictors of ecosystem function, however,
- Sub-dominant species in functional groups are not as strong predictors as key species are, suggesting that some functional groups may have less resilience and redundancy than assumed.
- Species which promote the regeneration and removal of inorganic nitrogen vary due to a complex combination of ecosystem variables and can provide important information on nutrient pathways within the Manukau Harbour.

While the results do not differentiate between the significance of functional groups or key species, they do support the idea that one key species dominates a functional role and the remaining species contribute less to ecosystem function. This has important connotations for redundancy and ecosystem resilience, which

facilitate management and protection of our estuaries and ecosystems in rapidly changing times

The knowledge and understanding of how nutrients are cycled, regenerated and removed from these ecosystems is key in managing our land use and the impact we are having on our estuaries, which can be sensitive to stressors or disturbances and are already under high levels of stress from anthropogenic sources. Understanding the removal of nitrogen is imperative for managing the amount of nitrogen we are discharging into harbours, especially with the current trends and issues in water quality both nationally and internationally.

## References

---

- Alberti J, Cebrian J, Alvarex F, Escapa M, Esquiús KS, Fanjul E, Sparks EL, Mortazavi B and Iribane O. (2017). *Nutrient and herbivore alterations cause uncoupled changes in producer diversity, biomass and ecosystem function, but not in overall multifunctionality*. Scientific Reports. 7, Article number: 2693.
- Aller RC. (1988). *Benthic fauna and biogeochemical processes in marine sediments: the role of burrow structures*. In Blackburn TH and Sørensen J (editors), *Nitrogen Cycling in Coastal Marine Environments*. John Wiley & Sons, England. Chapter 13, 301 – 338.
- Alonso-Pérez F and Castro CG. (2014). *Benthic oxygen and nutrient fluxes in a coastal upwelling system (Ria de Vigo, NW Iberian Peninsula): Seasonal trends and regulating factors*. Marine Ecology Progress Series. 511, 17 - 32.
- An S and Joye SB. (2001). *Enhancement of coupled nitrification-denitrification by benthic photosynthesis in shallow estuarine sediments*. Limnology and Oceanography. 46, 62 – 74.
- Anderson MJ. (2008). *Animal-sediment relationships re-visited: characterising species' distribution along an environmental gradient using canonical analysis and quantile regression splines*. Journal of Experimental Marine Biology and Ecology. 366, 16 - 27.
- Badesab F, von Döbeneck T, Briggs RM, Bryan KR, Just J and Müller H. (2017). *Sediment dynamics of an artificially deepened mesotidal coastal lagoon: an environmental magnetic investigation of Tauranga Harbour, New Zealand*. Estuarine, Coastal and Shelf Science. 194, 240 – 251.
- Barbier EB, Hacker SD, Kennedy C, Koch EW, Stier AC and Silliman BR. (2011). *The value of estuarine and coastal ecosystem services*. Ecological Monographs. 81, 169 - 193.
- Bartoli M, Nizzoli D, Welsh DT and Viaroli P. (2000). *Short-term influence of recolonisation by the polychaete worm Nereis succinea on oxygen and nitrogen fluxes and denitrification: a microcosm simulation*. Hydrobiologia. 431, 165 – 174.
- Berelson WM, McManus J, Severmann S and Reimers VE. (2013). *Benthic flux of oxygen and nutrients across Oregon/California shelf sediments*. Continental Shelf Research. 55, 66 – 75.
- Blondel J. (2003). *Guilds or functional groups: does it matter?* Oikos. 100, 223 – 231.
- Boyer JN, Christian RR and Stanley DW. (1993). *Patterns of phytoplankton primary productivity in the Neuse River Estuary, North Carolina, USA*. Marine Ecology Progress Series. 97, 287 – 297.



- Bremer S and Funtowicz S. (2015). *Negotiating a place for sustainability science: narratives from the Waikaraka Estuary in New Zealand*. Environmental Science and Policy. 53, 47 – 59.
- Bremner J, Rogers SI and Frid CLJ. (2003). *Assessing functional diversity in marine benthic ecosystems: a comparison of approaches*. Marine Ecological Progress Series. 254, 11 – 25.
- Butterfield BJ and Suding KN. (2012). *Single-trait functional indices outperform multi-trait indices in linking environmental gradients and ecosystem services in a complex landscape*. Journal of Ecology. 101, 9 – 17.
- Cameron WM and Pritchard DW. (1963). *Estuaries*. In M. N. Hill (editor), *The Sea*, John Wiley & Sons, New York. 2, 306 - 324.
- Cardinale BJ, Duffy JE, Gonzalez A, Hooper D, Perrings C, Venail P, Narwani A, Mace GM, Tilman D, Wardle DA, Kinzig AP, Daily GC, Loreau M, Grace JB, Larigauderie A, Srivastava DS and Naeem S. (2012). *Biodiversity and its impact on humanity*. Nature. 486, 59 – 67.
- Chapin III FS. (1993). *Functional role of growth forms in ecosystem and global processes*. In Roy J, Ehleringer JR and Field CB (editors), *Scaling Physiological Processes; Leaf to Globe*. Academic Press, Inc. San Diego, California, USA. Ch 16, 287 – 312
- Christensen JP, Devol AH and Smethie Jr. WM. (1984). *Biological enhancement of solute exchange between sediments and bottom water on the Washington continental shelf*. Continental Shelf Research. 3, 9 – 23.
- Cloern JE, Abreu PC, Carstensen J, Chavaud L, Elmgren R, Grall J, Greening H, Johansson JOR, Kahru M, Sherwood ET, Xu J and Yun K. (2015). *Human activities and climate variability drive fast-paced change across the world's estuarine-coastal ecosystems*. Global Change Biology. 2, 512 – 529.
- Decleyre H, Heylen K, Sabbe K, Tytgat B, Deforce D, Van Nieuwerburgh F, Van Colen C and Willems A. (2015). *A doubling of microphytobenthos biomass coincides with a tenfold increase in denitrifier and total bacterial abundances in intertidal sediments of a temperate estuary*. PLoS ONE. DOI:10.1371/journal.pone.0126583.
- Diaz S and Cabido M. (2001). *Vive la différence; plant functional diversity matters to ecosystem processes*. Trends in Ecology and Evolution. 16, 646 – 655.
- Dollar SJ, Smith SV, Vink SM, Obrebski S and Hollibaugh JT. (1991). *Annual cycle of benthic nutrient fluxes in Tomales Bay, California, and contribution of the benthos to total ecosystem metabolism*. Marine Ecology Progress Series. 79, 115 – 125.
- Duarte C and Chiscano CL. (1999). *Seagrass biomass and production: a reassessment*. Aquatic Botany. 65, 159 – 174.

- Ellingson KE, Hewitt JE and Thrush SF. (2006). *Rare species, habitat diversity and functional redundancy in marine benthos*. Journal of Sea Research. 58, 291 – 301.
- Espinosa F, Guerra-Garcia JM. (2005). *Algae, macrofaunal assemblages and temperature: a quantitative approach to intertidal ecosystems of Iceland*. Helgoland Marine Research. 59, 273 – 285.
- Fanjul E, Bazterrica MC, Escapa M, Grela MA and Iribarine O. (2011). *Impacts of crab bioturbation on benthic flux and nitrogen dynamics of Southwest Atlantic intertidal marshes and mudflats*. Estuarine, Coastal and Shelf Science. 92, 629 – 638.
- Fitzmaurice JR. (2009). *History of Auckland Wastewater and Mangere Wastewater Treatment Plant*. Paper presented at 3<sup>rd</sup> Australasian Engineering Heritage Conference 2009. 1 - 9. Accessed from [https://www.ipenz.org.nz/heritage/conference/papers/Fitzmaurice\\_J.pdf](https://www.ipenz.org.nz/heritage/conference/papers/Fitzmaurice_J.pdf) on 14/09/2017.
- Fry B, Rogers K, Barry B, Barr N and Dudley B. (2011). *Eutrophication indicators in the Hutt River Estuary, New Zealand*. New Zealand Journal of Marine and Freshwater Research. 45, 665 – 677.
- Gammal J, Norkko J, Pilditch CA and Norkko A. (2017). *Coastal hypoxia and the importance of benthic macrofauna communities for ecosystem functioning*. Estuaries and Coasts. 40, 457 – 468.
- Gitay H, Wilson JB and Lee WG. (1996). *Species redundancy: a redundant concept?* Journal of Ecology. 84, 121 – 124.
- Gladstone-Gallagher RV, Lohrer AM, Lundquist CJ and Pilditch CA. (2016). *Effects of detrital subsidies on soft-sediment ecosystem function are transient and source-dependent*. PLoS ONE. <https://doi.org/10.1371/journal.pone.0154790>.
- Gray JS. (1997). *Marine biodiversity: patterns, threats and conservation needs*. Biodiversity and Conservation. 6, 153 – 175.
- Green L and Fong P. (2015). *The good, the bad and the Ulva: the density dependent role of macroalgal subsidies in influencing diversity and trophic structure of an estuarine community*. Oikos. 125, 988 – 1000.
- Greenfield B, Hewitt J and Hailes S. (2013). *Manukau Harbour ecological monitoring program: report on data collected up until February 2013*. Prepared by NIWA for Auckland Regional Council. Auckland Regional Council technical report, TR2013/027.
- Greenfield BL, Kraan C, Pilditch CA and Thrush SF. (2016). *Mapping functional groups can provide insight into ecosystem functioning and potential resilience of intertidal sandflats*. Marine Ecology Progress Series. 548, 1 - 10.

- Griffiths JR, Kadin M, Nascimento FJA, Tamelander T, Törnroos A, Bonaglia S, Bonsdorff E, Brüchet V, Gårdmark A, Järnström M, Kotta J, Lindegren M, Nordström MC, Norkko A, Olsson J, Weigel B, Žydelis R, Blenckner T, Niiranen S, Winder M. (2017). *The importance of benthic-pelagic coupling for marine ecosystem functioning in a changing world*. *Global Change Biology*. 23, 2179 – 2196.
- Grundmanis V and Murray JW. (1977). *Nitrification and denitrification in marine sediments from Puget Sound*. *Limnology and Oceanography*. 22, 804 – 813.
- Gunderson LH. (2000). *Ecological resilience – in theory and application*. *Annual Review of Ecology, Evolution and Systematics*. 31, 425 – 439.
- Hamersley MR and Howes BL. (2005). *Evaluation of the N<sub>2</sub> flux approach for measuring sediment denitrification*. *Estuarine, Coastal and Shelf Science*. 62, 711 – 723.
- Hanisak MD. (1983). *The nitrogen relationships of marine microalgae*. In Carpenter EJ and Capone DG (editors), *Nitrogen in the Marine Environment*. Academic Press, New York, USA. 699 – 730.
- Harris RJ, Pilditch CA, Hewitt JE, Lohrer AM, Van Colen C, Townsend M and Thrush SF. (2015). *Biotic interactions influence sediment erodibility on wave-exposed sandflats*. *Marine Ecology Progress Series*. 523, 15 – 30.
- Haughtier Y, Niklaus PA and Hector A. (2009). *Competition for light causes plant biodiversity loss after eutrophication*. *Science*. 324, 363 – 368.
- Heath RA. (1976). *Broad classification of New Zealand inlets with emphasis on residence times*. *New Zealand Journal of Marine and Freshwater Research*. 10, 429 – 444.
- Henderson I. (Photographer). (2006). *Aerial photograph of oxidation settling ponds in the Manukau Harbour before and after removal*. Retrieved from <https://www.nzgeo.com/stories/manukau-harbour/>.
- Henriksen K and Kemp WM. (1988). *Nitrification in estuarine and coastal marine sediments*. In Blackburn TH and Sørensen J (editors), *Nitrogen Cycling in Coastal Marine Environments*. John Wiley & Sons, New York, USA. Chapter 10, 207 – 240.
- Henriksen K, Rasmussen MB and Jensen A. (1983). *Effect of bioturbation on microbial nitrogen transformations in the sediments and fluxes of ammonium and nitrate to the overlying water*. *Environmental biogeochemistry*. 35, 195 – 205.
- Herbert RA. (1999). *Nitrogen cycling in coastal marine ecosystems*. *FEMS Microbiology Reviews*. 23, 563 – 590.
- Hesp PA, Shepherd MJ and Parnell K. (1999). *Coastal geomorphology in New Zealand, 1989-99*. *Progress in Physical Geography*. 23, 501 – 524.

- Hewitt J, Thrush S, Lohrer A and Townsend M. (2010). *A latent threat to biodiversity: consequences of small-scale heterogeneity loss*. Biodiversity Conservation. 19, 1315 – 1323.
- Hewitt JE, Thrush SF and Ellingsen KE. (2016). *The role of time and species indentities in spatial patterns of species richness and conservation*. Conservation Biology. 30, 1080 - 1088
- Hochard S, Pinazo C, Grenz C, Burton Evans JL and Pringault O. (2010). *Impact of microphytobenthos on the sediment biogeochemical cycles: a modelling approach*. Ecological Modelling. 221, 1697 – 1701.
- Hopkinson Jr. CS, Giblin AE, Tucker J, and Garrit RH. (1999). *Benthic metabolism and nutrient cycling along an estuarine salinity gradient*. Estuaries. 22, 863 – 891.
- Houde ED and Rutherford ES. (1993). *Recent trends in estuarine fisheries: predictions of fish production and yield*. Estuaries. 16, 161 – 176.
- Huettel M, Ziebis W, Forster A and Luther III GW. (1998). *Advective transport affecting metal and nutrient distributions and interfacial fluxes in permeable sediments*. Geochimica et Cosmochimica Acta. 62, 613 – 631.
- Hume TM, Bell RG, de Lange W, Healy TR, Hicks DM and Kirk RM. (1992). *Coastal oceanography and sedimentology in New Zealand, 1967 – 91*. New Zealand Journal of Marine and Freshwater Research. 26, 1 – 36.
- Hume TM and Herdendorf CE. (1988). *A geomorphic classification of estuaries and its application to coastal resource management – a New Zealand example*. Ocean and Shoreline Management. 11, 249 – 274.
- Hume TM and Herdendorf CE. (1993). *On the use of empirical stability relationships for characterising estuaries*. Journal of Coastal Research. 9, 413 – 422.
- Hutchinson GE. (1959). *Homage to Santa Rosalia or why are there so many kinds of animals?* American Naturalist. 870, 145 – 159.
- Jackson JBC, Kirby MX, Berger WH, Bjorndal KA, Botsford LW, Bourque BJ, Bradbury RH, Cooke R, Eslandson J, Estes JA, Hughes TP, Kidwell S, Lange CB, Lenihan HS, Pandolfi JM, Peterson CH, Steneck RS, Tegner MJ and Warner RR. (2001). *Historical overfishing and the recent collapse of coastal ecosystems*. Science, 293, 629 – 637.
- Jain M, Flynn DFB, Prager CM, Hart GM, DeVan CM, Ahrestani FS, Palmer MI, Bunker DE, Knops JMH, Jouseau CF and Naeem S. (2013). *The importance of rare species a trait-based assessment of rare species contributions to functional diversity and possible ecosystem function in tall-grass prairies*. Ecology and Evolution. 4, 14 – 112.

- Ji T, Du J, Moore WS, Zhang G, Su N and Zhang J. (2013). *Nutrient inputs to a lagoon through submarine groundwater discharge: the case of Laoye Lagoon, Hainan, China*. Journal of Marine Systems. 111, 253 – 262.
- Johannes RE and Hearn CJ. (1985). *The effect of submarine groundwater discharge on nutrient and salinity regimes in a coastal lagoon off Perth, Western Australia*. Estuarine, Coastal and Shelf Science. 21, 789 – 800.
- Joint IR. (1978). *Microbial production of an estuarine mudflat*. Estuarine and Coastal Marine Science. 7, 185 – 195.
- Jones HFE, Pilditch CA, Hamilton DP and Bryan KR. (2017). *Impacts of a bivalve mass mortality event on an estuarine food web and bivalve grazing pressure*. New Zealand Journal of Marine and Freshwater Research. 51, 370 – 392.
- Jordan MA, Welsh DT, Junn RJK and Teasdale PR. (2009). *Influence of Trypaea australiensis population density on benthic metabolism and nitrogen dynamics in sandy estuarine sediment: a mesocosm simulation*. Journal of Sea Research. 61, 144 – 152.
- Kelahar BP and Levinton JS. (2003). *Variation in detrital enrichment causes spatio-temporal variation in soft-sediment assemblages*. Marine Ecology Progress Series. 261, 85 – 97.
- Kelly S. (2008). *Environmental condition and values of Manukau Harbour*. Prepared by Coast and Catchment Ltd. For Auckland Regional Council. Auckland Regional Council Technical Report 2009/1 12. Auckland City, New Zealand.
- Kelly S. (2014). *Mangere Wastewater Treatment Plant: Harbour Monitoring 2013 - 14*. Client report for Watercare Services Ltd., Coast and Catchment Ltd., Auckland. Auckland City, New Zealand.
- Kennedy DM and Dickson ME. (2007). *Cliffed coasts of New Zealand: perspectives and future directions*. Journal of the Royal Society of New Zealand. 32, 41 – 57.
- Komorita T, Tsutsumi H, Kajihara R, Suga N, Shibamura A, Yamada T and Montani S. (2012). *Oceanic nutrient supply and uptake by microphytobenthos of the Hichirippu Lagoon, Hokkaido, Japan*. Marine Ecology Progress Series. 446, 161 – 171.
- Kristensen E, Anderson FØ and Blackburn TH. (1992). *Effects of benthic macrofauna and temperature on degradation of macroalgal detritus: the fate of organic carbon*. Limnology and Oceanography. 37, 1404 – 1419.
- Laverock B, Gilbert JA, Tait K, Osborn AM and Widdicombe S. (2011). *Bioturbation: impact on the marine nitrogen cycle*. Biochemical Society Transactions. 39, 315 – 320.

- Levinton JS and Stewart S. (1988). *Effects of sediment organics, detrital input, and temperature on demography, production, and body size of a deposit feeder*. Marine Ecology Progress Series. 49, 259 – 266.
- Lohrer AM, Thrush SF and Gibbs MM. (2004). *Bioturbators enhance ecosystem function through complex biogeochemical interactions*. Letters to Nature. 431, 1092 – 1095.
- Lohrer AM, Thrush SF, Hewitt JE and Kraan C. (2015). *The up-scaling of ecosystem functions in a heterogeneous world*. Scientific reports. 5, 10349. doi:10.1038/srep10349.
- Lohrer AM, Thrush SF, Hunt L, Hancock N and Lundquist C. (2005). *Rapid reworking of subtidal sediments by burrowing spatangoid urchins*. Journal of Experimental Marine Biology and Ecology. 321, 155 – 169.
- Lohrer AM, Townsend M, Hailes SF, Rodil IF, Cartner K, Pratt DR and Hewitt JE. (2016). *Influence of New Zealand cockles (Austrovenus stutchburyi) on primary productivity in sandflat-seagrass (Zostera muelleri) ecotones*. Estuarine, Coastal and Shelf Science. 181, 238 – 248.
- Lohrer AM, Townsend M, Rodil IF, Hewitt JE and Thrush SF. (2012). *Detecting shifts in ecosystem functioning: the decoupling of fundamental relationships with increased pollutant stress on sandflats*. Marine Pollution Bulletin. 64, 2761 – 2769.
- Lohse L, Epping EHG, Helder W and van Raaphorst W. (1996). *Oxygen pore water profiles in continental shelf sediments of the North Sea: turbulent versus molecular diffusion*. Marine Ecology Progress Series. 145, 63 – 75.
- Loreau M, Naeem S, Inchausti P, Bengtsson J, Grime JP, Hector A, Hooper Du, Huston MA, Raggaellii D, Schmid B, Tilman D and Wardle DA. (2001). *Biodiversity and ecosystem functioning: current knowledge and future challenges*. Science. 294, 804 – 808.
- Lotze HK and Milewski I. (2004). *Two centuries of multiple human impacts and successive changes in a North Atlantic food web*. Ecological Applications. 14, 1428 – 1447.
- Macreadie PI, Ross DJ, Longmore AR and Keough MJ. (2006). *Denitrification measurements of sediments using cores and chambers*. Marine Ecology Progress Series. 326, 49 - 56.
- Marsden IS and Adkins SC. (2007). *Current status of cockle bed restoration in New Zealand*. Aquaculture International. 18, 83 – 97.
- Mayer MS, Schaffner L and Kemp WM. (1995). *Nitrification potentials of benthic macrofaunal tubes and burrow walls: effects of sediment  $\text{NH}_4^+$  and animal irrigation behaviour*. Marine Ecology Progress Series. 121, 157 – 169.

- McCartain LD, Townsend M, Thrush SF, Wetthey DS, Woodin SA, Volkenborn N and Pilditch CA. (2017). *The effects of thin mud deposits on the behaviour of a deposit-feeding tellinid bivalve: implications for ecosystem functioning*. Marine and Freshwater Behaviour and Physiology. 50, 239 – 255.
- Moncreiff CA, Sullivan MJ and Daehnick AE. (1992). *Primary production dynamics in seagrass beds of Mississippi Sound: the contributions of seagrass, epiphytic algae, sand microflora, and phytoplankton*. Marine Ecology Progress Series. 87, 161 – 171.
- Morar SR, Bury SJ, Wilkinson SP and Davy SK. (2011). *Sedimentary nitrogen uptake and assimilation in the temperate zooxanthellate sea anemone Anthopleura aureoradiata*. Journal of experimental Marine Biology and Ecology. 399, 110 – 119.
- Murray F, Douglas A and Solan M. (2014). *Species that share traits do not necessarily form distinct and universally applicable functional effect groups*. Marine Ecology Progress Series. 516, 23 – 34.
- Naeem S, Loreau M and Inchausti P. (2002). *Biodiversity and ecosystem functioning the emergence of a synthetic ecological framework*. In Naeem S, Loreau M and Inchausti P (editors), *Biodiversity and Ecosystem functioning*. Oxford University Press, Oxford, England. Chapter 1, 3 – 11.
- Needham HR, Pilditch CA, Lohrer AM and Thrush SF. (2011). *Context-specific bioturbation mediates changes to ecosystem functioning*. Ecosystems. 14, 1096 – 1109.
- Niemi GJ, DeVore P, Detenbeck N, Taylor D, Lima A, Pastor J, Yount JD and Naiman RJ. (1990). *Overview of case studies on recovery of aquatic systems from disturbance*. Environmental management. 14, 571 – 587.
- Ní Longphuirt S, Lim J, Leynaert A, Claquin P, Choy E, Kang C and An S. (2009). *Dissolved inorganic nitrogen uptake by intertidal microphytobenthos: nutrient concentrations, light availability and migration*. Marine Ecology Progress Series. 379, 33 – 44.
- Nilsson P and Jansson M. (2002). *Hydrodynamic control of nitrogen and phosphorus turnover in an eutrophicated estuary in the Baltic*. Water Research. 36, 4616 – 4626.
- Norkko A, Villnäs A, Norkko J, Valanko S and Pilditch C. (2013). *Size matter: implications of the loss of large individuals for ecosystem function*. Scientific Reports. 3, article no. 2646. doi:10.1038/srep02646.
- Norling K, Roseberg R, Hulth S, Grémare A and Bonsdorff E. (2007). *Importance of functional diversity and species-specific traits of benthic fauna for ecosystem functions in marine sediment*. Marine Ecology Progress Series. 332, 11 – 23.

- Nowicki BL. (1994). *The effect of temperature, oxygen, salinity, and nutrient enrichment on estuarine denitrification rate measured with a modified nitrogen gas flux technique*. Estuarine, Coastal and Shelf Science. 38, 137 – 156.
- O'Meara TA, Hillman JR and Thrush SF. (2017). *Rising tides, cumulative impacts and cascading changes to estuarine ecosystem functions*. Scientific Reports. 7, Article number: 10218. doi:10.1038/s41598-017-11058-7.
- Patrick CJ and Swan CM. (2011). *Reconstructing the assembly of a stream-insect metacommunity*. Journal of the North American Benthological Society. 30, 259 – 272.
- Pelegri SP, Nielsen LP and Blackburn TH. (1994). *Denitrification in estuarine sediment stimulated by the irrigation activity of the amphipod Corophium volutator*. Marine Ecology Progress Series. 105, 285 – 290.
- Pendleton RM, Horinghaus DJ, Gomes LC and Agostinho AA. *Loss of rare fish species from tropical floodplain food webs affects community structure and ecosystem multifunctionality in a mesocosm experiment*. PLoS ONE, <https://doi.org/10.1371/journal.pone.0084568>.
- Perez BC, Day Jr. JW, Justic D, Lane RR and Twilley RR. (2011). *Nutrient stoichiometry, freshwater residence time, and nutrient retention in a river-dominated estuary in the Mississippi delta*. Hydrobiologia. 658, 41 – 54.
- Poppe LJ, Eliason AH, Fredericks JJ, Rendigs RR, Blackwood D and Polloni CF. (2000). USGS East-coast sediment analysis: procedures, database, and georeferenced displays. *Chapter 1: Grain-size analysis of marine sediments – methodology and data processing*. U.S. Geological Survey Open-File Report 00-358. U.S. Geological Survey, Centre for Coastal and Marine Geology, Woods Hole, MA, USA.
- Risgaard-Petersen, N. (2004). *Denitrification*. In Neilsen S, Banta G and Pederson M (editors), *Estuarine Nutrient Cycling: The Influence of Primary Producers*. Kluwer Academic Publishers, Netherlands. 263 – 280.
- Robertson BP, Gardner JPA and Savage C. (2015). *Macrobenthic-mud relations strengthen the foundation for benthic index development: a case study from shallow, temperate New Zealand Estuaries*. Ecological Indicators. 58, 161 – 174.
- Rodil IF, Lohrer AM, Hewitt JE, Townsend M, Thrush SF and Carbines M. (2013). *Tracking environmental stress gradients using three biotic integrity indices: advantages of locally-developed traits-based approach*. Ecological Indicators. 34, 560 – 570.
- Rönner U. (1985). *Nitrogen transformation in the Baltic proper: denitrification counteracts eutrophication*. Ambio. 14, 134 – 138.



- Sakamaki T, Nishimura O and Sudo R. (2006). *Tidal time-scale variation in nutrient flux across the sediment-water interface of an estuarine tidal flat*. Estuarine, Coastal and Shelf Science. 67, 653 – 663.
- Sandwell DR, Pilditch CA and Lohrer AM. (2009). *Density dependent effects of an infaunal suspension-feeding bivalve (Austrovenus stutchburyi) on sandflat nutrient fluxes and microphytobenthic productivity*. Journal of Experimental Marine Biology and Ecology. 373, 16 – 25.
- Sartory DP. (1982). *Spectrophotometric analysis of chlorophyll a in freshwater phytoplankton*. Hydrological research institute. TR 115. Department of environmental affairs, Pretoria, South Africa.
- Schleuter D, Daufresne M, Massol F and Argillier C. (2001). *A user's guide to functional diversity indices*. Ecological Monographs. 80, 469 – 484.
- Seitzinger SP. (1988). *Denitrification in freshwater and coastal marine ecosystems: ecological and geochemical significance*. American Society of Limnology and Oceanography. 33, 702 – 724.
- Simberloff D and Dayan T. (1991). *The guild concept and the structure of ecological communities*. Annual Review of Ecology and Systematics. 22, 115 – 143.
- Smith MD and Knapp AK. (2003). *Dominant species maintain ecosystem function with non-random species loss*. Ecology Letters. 6, 509 – 517.
- Strong JA, Andonegi E, Bizsel KC, Danovaro R, Elliot M, Franco A, Garces E, Little S, Mazik K, Moncheva S, Papadopoulou N, Patrício J, Queirós AM, Smith C, Stefanova K and Solaun O. (2015). *Marine biodiversity and ecosystem function relationships: the potential for practical monitoring applications*. Estuarine, Coastal and Shelf Science. 161, 46 – 64.
- Sundback K, Linares F, Larson F, Wulff A and Engelsen A. (2004). *Benthic nitrogen fluxes along a depth gradient in a microtidal fjord: the role of denitrification and microphytobenthos*. Limnology and Oceanography. 49, 1095 – 1107.
- Sundback K, Miles A and Göransson E. (2000). *Nitrogen fluxes, denitrification and the role of microphytobenthos in microtidal shallow-water sediments: an annual study*. Marine Ecology Progress Series. 200, 59 – 76.
- Svensson JM and Leonardson L. (1996). *Effects of bioturbation by tube-dwelling chironomid larvae on oxygen uptake and denitrification in eutrophic lake sediments*. Freshwater Biology. 35, 289 – 300.
- Syvitski JPM, Vörösmarty CJ, Kettner AJ and Green P. (2005). *Impact of humans on the flux of terrestrial sediment to the global coastal ocean*. Science. 308, 376 – 380.
- Taylor SL, Bishop MJ, Kelager BP and Glasby TM. (2010). *Impacts of detritus from the invasive alga Caulerpa taxifolia on a soft sediment community*. Marine Ecology Progress Series. 420, 73 – 81.

- Teichberg M, Fox SE, Olsen YS, Valiela I, Martinetto P, Iribarne O, Muto EY, Petti MAV, Corbisier TN, Soto-Jiminez M, Paez – Osuna F, Castro P, Freitas H, Zitelli A, Cardinaletti M and Tagliapeitra D. (2010). *Eutrophication and macroalgal blooms in temperate and tropical coastal waters: nutrient enrichment experiments with Ulva spp.* Global Change Biology. 16, 2624 – 2637.
- Teichert N, Lepage M, Sagouis A, Borja A, Chust G, Ferriera MT, Pasquaud S, Schinegger R, Segurado P and Argillier C. (2017). *Functional redundancy and sensitivity of fish assemblages in european rivers, lakes and estuarine ecosystems.* Scientific Reports. 7, article no. 17611. doi:10.1038/s41598-017-17975-x.
- Thrush SF, Halliday J, Hewitt JE and Lohrer AM. (2008). *The effects of habitat loss, fragmentation, and community homogenization on resilience in estuaries.* Ecological Applications. 18, 12 – 21.
- Thrush SF, Hewitt JE, Gibbs M, Lundquist C and Norkko A. (2006). *Functional role of large organisms in intertidal communities: community effects and ecosystem function.* Ecosystems. 9, 1029 – 1040.
- Thrush SF, Townsend M, Hewitt JE, Davies K, Lohrer AM, Lundquist C and Cartner K. (2013). *The many uses and values of estuarine ecosystems.* In Dymond JR (editor), *Ecosystem services in New Zealand – Conditions and trends.* Manaaki Whenua Press, Lincoln, New Zealand.
- Tilman D, Wedin D and Knops J. (1991). *Productivity and sustainability influenced by biodiversity in grassland ecosystems.* Letters to Nature. 379, 718 – 720.
- Törnroos A and Bonsdorff E. (2012). *Developing the multitrait concept for functional diversity: lessons from a system rich in functions but poor in species.* Ecological Applications. 22, 2221 – 2236.
- Valle-Levinson A. (2011). *Definition and classification of estuaries.* In Contemporary Issues in Estuarine Physics. Cambridge University Press, Cambridge, United Kingdom. 1 – 11. <https://doi.org/10.1017/CBO9780511676567.002>.
- Van Colen C, Thrush SF, Parkes S, Harris R, Wooden SA, Wethey DS, Pilditch CA, Hewitt JE, Lohrer AM and Vincx M. (2015). *Bottom-up and top-down mechanisms indirectly mediate interactions between benthic biotic ecosystem components.* Journal of Sea Research. 98, 42 – 48.
- Varela M and Penas E. (1985). *Primary production of benthic microalgae in an intertidal sand flat of the Ria de Arosa, NW Spain.* Marine Ecology Progress Series. 25, 111 – 119.
- Villnäs A, Hewitt J, Snickars M, Westerborn M and Norkko A. (2017). *Template for using biological trait groupings when exploring large-scale variation in seafloor multifunctionality.* Ecological applications. 28, 78 – 94.

- Vincent B, Joly D and Harvey M. (1994). *Spatial variation in growth of the bivalve Macoma balthica (L.) on a tidal flat: effects of environmental factors and intraspecific competition*. Journal of Experimental Marine Biology and Ecology. 181, 223 – 238.
- Val Klump J and Martens CS. (1987). *Biogeochemical cycling in an organic-rich coastal marine basin. 5. Sedimentary nitrogen and phosphorus budgets based upon kinetic models, mass balances, and the stoichiometry of nutrient regeneration*. Geochimica et Cosmochimica Acta. 51, 1161 – 1173.
- Vitousek PM, Aber JD, Howarth RW, Likens GE, Matson PA, Schindler DW, Schlesinger WH and Tilman DG. (1997). *Human alteration of the global nitrogen cycle: sources and consequences*. Ecological Applications. 7, 737 – 750.
- Vitousek PM, Mooney HA, Lubchenco J and Melillo JM. (1997). *Human domination of Earth's Ecosystems*. Science. 277, 494 – 499.
- Volkenborn N, Meile C, Polerecky L, Pilfitch CA, Norkko A, Norkko J, Hewitt JE, Thrush SF, Wethey DS and Woodin SA. (2012). *Intermittent bioirrigation and oxygen dynamics in permeable sediments: and experimental and modelling study of three tellinid bivalves*. Journal of Marine Research. 70, 794 – 823.
- Watercare Services Ltd. (Photographer). Date unknown. *Manukau Harbour catchment with nearby towns/regions*. Retrieved from [www.watercare.co.nz](http://www.watercare.co.nz)
- Webb AP and Eyre BD. (2004). *Effect of natural populations of burrowing thalassinidea shrimp on sediment irrigation, benthic metabolism, nutrient fluxes and denitrification*. Marine Ecology Progress Series. 268, 205 – 220.
- Webb JE and Theodor J. (1968). *Irrigation of submerged marine sands through wave action*. Nature. 220, 682 – 685.
- Whitlatch RB. (1981). *Animal-sediment relationships in intertidal marine benthic habitats: some determinants of deposit-feeding species diversity*. Journal of Experimental Marine Biology and Ecology. 53, 31 – 45.
- Wild-Allen K and Andrewartha J. (2016). *Connectivity between estuaries influences nutrient transport, cycling and water quality*. Marine chemistry. 185, 12 – 26.
- Williamson RB, Blom A, Hume TM and Gladsby GP. (1992). *Heavy Metals in the Manukau Harbour sediments*. Water Quality publication 23. Water Quality Centre, Hamilton, DSIR. ISBN 0-477-02653-2. Hamilton, New Zealand.
- Wilson JB. (1999). *Guilds, functional types and ecological groups*. Oikos. 86, 507 – 522.

Woodin SA, Volkenborn N, Pilditch CA, Logrer AM, Wethey DS, Hewitt Je and Thrust SF. (2015). *Same pattern, different mechanism: locking onto the role of key species in seafloor ecosystem process*. Scientific reports. 6, article no. 26678. doi:10.1038/srep26678.

Woods LM, Biro EG, Yang M and Smith KG. (2016). *Does regional diversity recover after disturbance? A field experiment in constructed ponds*. PeerJ. 10.7717/peerj.2455.

# Appendices

## Appendix 1

Species	Functional group number	Functional group code	Core sample occurrence	Site occurrence	Total n
<i>Austrominius modestus</i>	1	BEI	16	4	38
<i>Austrovenus stutchburyi</i>	2	BEKN	55	5	988
<i>Paphies australis</i>	2	BEKN	10	1	52
<i>Hiatula siliquens</i>	3	BEKO	8	3	12
<i>Diplodonta australis</i>	3	BEKO	4	1	4
<i>Arcuatula senhousia</i>	4	BEKP	1	1	1
<i>Notoacmea scapha</i>	5	BF/G/HJN	38	4	155
<i>Zeacumantus lutulentus</i>	5	BF/G/HJN	25	3	42
<i>Diloma subrostrata</i>	5	BF/G/HJN	17	3	31
<i>Cominella glandiformis</i>	5	BF/G/HJN	11	3	29
<i>Chiton glaucus</i>	5	BF/G/HJN	4	2	5
<i>Cantharidus tenebrosus</i>	5	BF/G/HJN	3	1	3
<i>Haminoea zelandiae</i>	5	BF/G/HJN	1	1	1
<i>Turbonilla sp.</i>	6	BF/GKN	2	2	2
<i>Linucula hartvigiana</i>	7	BFKO	51	4	625
<i>Lasaea parengaensis</i>	7	BFKO	12	2	78
<i>Arthritica bifurca</i>	7	BFKO	17	4	46
<i>Macomona liliana</i>	8	BFMOTW	78	6	766
<i>Cyclomactra ovata</i>	8	BFMOTW	11	3	14
<i>Anthopleura aureoradiata</i>	9	CEI	62	6	647
<i>Boccardia syrtis</i>	10	CEQ	34	5	67
<i>Phoronid sp.</i>	10	CEQ	18	2	40
<i>Travisia olens</i>	11	CFKN	9	1	20
<i>Orbinia papillosa</i>	12	CFLN	27	6	90
<i>Scoloplos cylindrifer</i>	12	CFLN	19	4	27
<i>Taeniogyrus dendyi</i>	12	CFLN	10	5	16
<i>Scolecopides benhami</i>	12	CFLN	11	4	12
<i>Microspio maori</i>	12	CFLN	6	2	9
<i>Aonides trifida</i>	13	CFLO	50	4	3415
<i>Heteromastus filiformis</i>	13	CFLO	72	6	1405
<i>Magelona dakini</i>	13	CFLO	67	6	660
<i>Prionospio aucklandica</i>	13	CFLO	31	6	490
<i>Paradoneis lyra</i>	13	CFLO	55	6	292
<i>Aricidea sp</i>	13	CFLO	31	6	62
<i>Cossura consimilis</i>	13	CFLO	4	1	4
<i>Levinsenia gracilis</i>	13	CFLO	2	1	2
<i>Prionospio cirrefera</i>	13	CFLO	2	2	2
<i>Capitella spp</i>	13	CFLO	1	1	1
<i>Prionospio ehlersi</i>	13	CFLO	1	1	1

<i>Macroclymenella stewartensis</i>	14	CFQ	24	3	156
<i>Owenia petersenae</i>	14	CFQ	28	4	60
<i>Psuedopolydora corniculata</i>	14	CFQ	11	2	20
<i>Psuedopolydora paucibranchiata</i>	14	CFQ	7	1	9
<i>Pectinaria australis</i>	14	CFQ	3	1	3
<i>Asychis sp</i>	14	CFQ	2	1	2
<i>Polydora</i>	14	CFQ	1	1	1
<i>Syllinae BC</i>	15	GCK/LO	19	2	53
<i>Oligochaeta</i>	15	CGK/LO	9	3	17
<i>Hesionidae</i>	15	CGK/LO	6	1	9
<i>Edwardsia sp.</i>	15	CGK/LO	1	1	1
<i>Dorvilleidae</i>	16	CGKN	2	2	2
<i>Pelogenia antipodium</i>	16	CGKN	1	1	1
<i>Nemertean</i>	17	CGL/MNT	47	6	85
<i>Sphaerosyllis semiverrucosa</i>	17	CGL/MNT	17	5	47
<i>Perinereis vallata</i>	17	CGL/MNT	18	3	30
<i>Ceratonereis</i>	17	CGL/MNT	14	2	21
<i>Nicon aestuariensis</i>	17	CGL/MNT	15	4	15
<i>Aglaophamus macroura</i>	17	CGL/MNT	9	3	11
<i>Glycera americana</i>	17	CGL/MNT	7	3	8
<i>Platynereis australis</i>	17	CGL/MNT	5	2	5
<i>Glycinde trifida</i>	17	CGL/MNT	5	3	5
<i>Diopatra sp</i>	18	CGLPQ	4	2	4
<i>Torridoharpinia hurleyi</i>	19	DF/GKNT	39	6	126
<i>Paracalliope novizealandiae</i>	19	DF/GKNT	22	5	55
<i>Methalimedes sp.</i>	19	DF/GKNT	10	2	21
<i>Phoxocephalidae spSE</i>	19	DF/GKNT	10	4	13
<i>protohyale</i>	19	DF/GKNT	9	3	11
<i>Urothoidae</i>	19	DF/GKNT	7	2	10
<i>Tanaidacea</i>	19	DF/GKNT	6	1	8
<i>Waitangi brevirostris</i>	19	DF/GKNT	4	2	6
<i>Paramoera cheveraux</i>	19	DF/GKNT	3	1	4
<i>Isocladus sp.</i>	19	DF/GKNT	1	1	1
<i>Philocheras australis</i>	19	DF/GKNT	1	1	1
<i>Hemiplax hirtipes</i>	20	DGLNS	9	4	9
<i>Austrohelice crassa</i>	20	DGLNS	1	1	2
<i>Colurostylis lemorum</i>	21	DJN	43	6	215
<i>Halicarcinus whitei</i>	21	DJN	41	6	92
<i>Cyclapsis thomsoni</i>	21	DJN	7	1	9
<i>Exosphaeroma planulum</i>	21	DJN	4	2	4
<i>Exosphaeroma waitemata</i>	21	DJN	2	1	2

## Appendix 2

	AA	CB	CH	EB	KP	PI	Total animals	% of total	No. of species	Sites present
CFLO*	307	680	603	791	1308	2645	6334	56.01	11	6
BEKN*	173	8	0	46	129	684	1040	9.20	2	5
BFMOTW*	144	63	12	47	214	300	780	6.90	2	6
BFKO*	78	159	0	3	93	416	749	6.62	3	5
CEI*	1	253	9	18	65	301	647	5.72	1	6
DJN*	162	31	26	27	43	33	322	2.85	5	6
BF/G/HJN	6	1	0	24	61	174	266	2.35	7	5
DEF/GKNT	23	111	12	37	50	23	256	2.26	11	6
CFQ*	0	227	8	0	12	4	251	2.22	7	5
CGL/MNT	11	32	23	11	71	79	227	2.01	9	6
CFLN	66	5	6	20	33	24	154	1.36	5	6
CEQ	6	80	3	0	17	1	107	0.95	2	5
CGK/LO	0	50	16	1	0	13	80	0.71	4	4
BEI	10	0	0	17	7	4	38	0.34	1	4
CFKN	20	0	0	0	0	0	20	0.18	1	1
BEKO	8	5	0	0	3	0	16	0.14	2	3
DGLNS	0	1	0	2	1	7	11	0.10	2	4
CGLPQ	0	2	2	0	0	0	4	0.04	1	2
CGKN	1	1	0	0	0	1	3	0.03	2	3
BF/GKN	0	1	0	0	1	0	2	0.02	1	2
BEKP	0	0	0	0	1	0	1	0.01	1	1
Total FG	15	18	11	13	17	16				
Total animals	1016	1710	720	1044	2109	4709	11308			

Functional groups annotated with \* are the groups used in each analysis.